LEVEL II

9

DTNSRDC-79/064 DESIGN EQUATIONS FOR TRIPPING OF STIFFENERS UNDER INPLANE AND LATERAL LOADS

DAVID W. TAYLOR NAVAL SHIP
RESEARCH AND DEVELOPMENT CENTER

Bethesda, Md. 20084

AD A074752

DESIGN EQUATIONS FOR TRIPPING OF STIFFENERS UNDER INPLANE AND LATERAL LOADS

by

John C. Adamchak

D D C
OCT 8 1979
E

APPROVED FOR PUBLIC RELEASE: DISTRIBUTION UNLIMITED

DDC FILE COPY

STRUCTURES DEPARTMENT
RESEARCH AND DEVELOPMENT REPORT

October 1979

DTNSRDC-79/064

79 10 05 029

MAJOR DTNSRDC ORGANIZATIONAL COMPONENTS

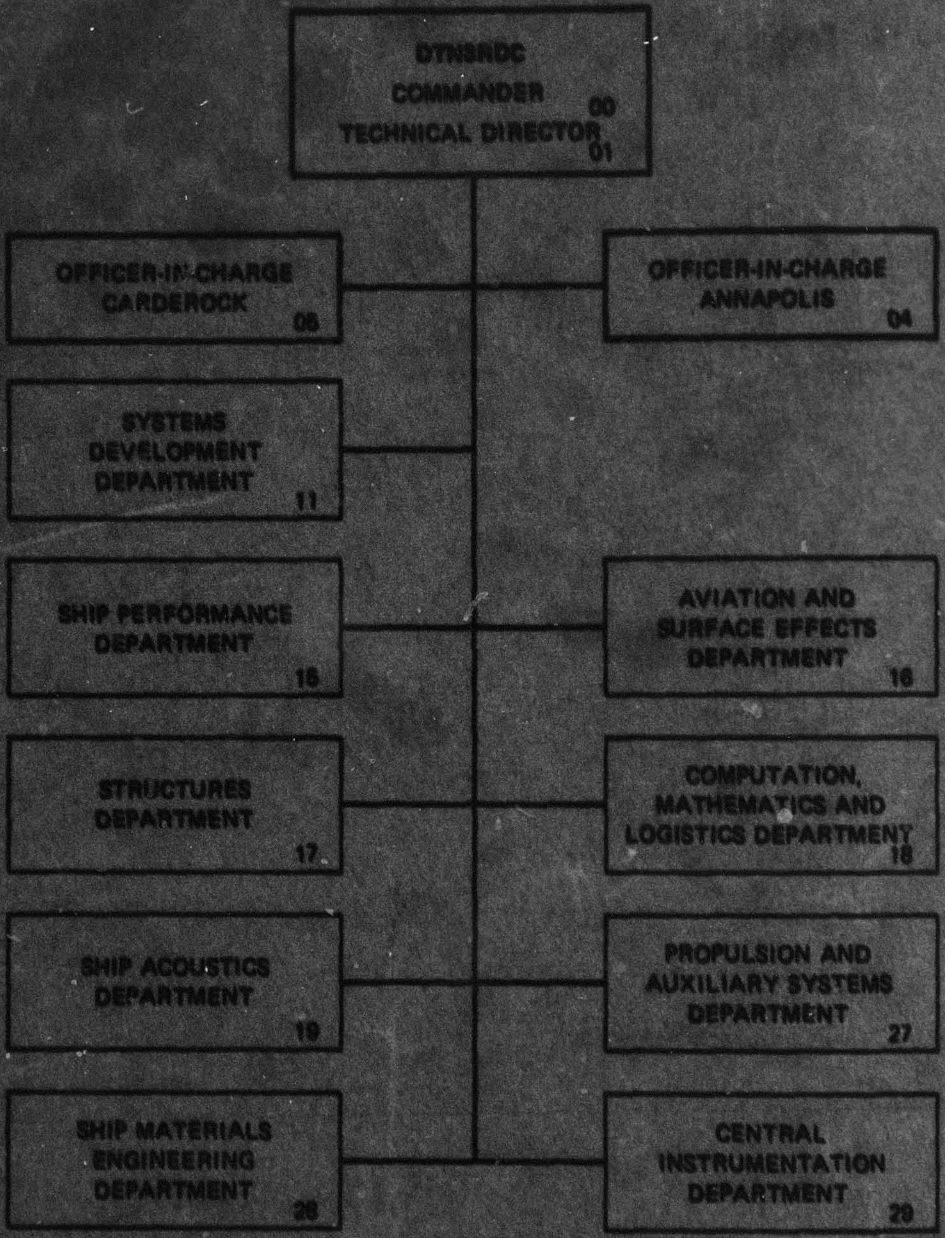
DTNSRDC
COMMANDER 00
TECHNICAL DIRECTOR 01
OFFICER-IN-CHARGE CARDEROCK 05
OFFICER-IN-CHARGE ANNAPOLIS 04
SYSTEMS DEVELOPMENT DEPARTMENT 11
SHIP PERFORMANCE DEPARTMENT 15
AVIATION AND SURFACE EFFECTS DEPARTMENT 16
STRUCTURES DEPARTMENT 17
COMPUTATION, MATHEMATICS AND LOGISTICS DEPARTMENT 18
SHIP ACOUSTICS DEPARTMENT 19
PROPULSION AND AUXILIARY SYSTEMS DEPARTMENT 27
SHIP MATERIALS ENGINEERING DEPARTMENT 28
CENTRAL INSTRUMENTATION DEPARTMENT 29

DISCLAIMER NOTICE

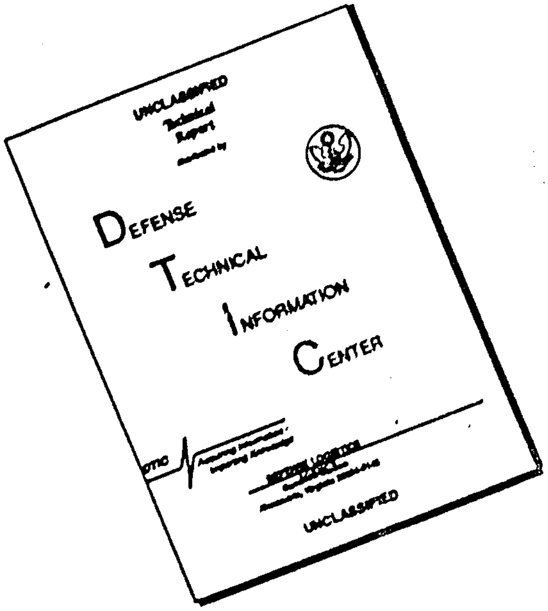

UNCLASSIFIED

DEFENSE TECHNICAL INFORMATION CENTER

UNCLASSIFIED

THIS DOCUMENT IS BEST QUALITY AVAILABLE. THE COPY FURNISHED TO DTIC CONTAINED A SIGNIFICANT NUMBER OF PAGES WHICH DO NOT REPRODUCE LEGIBLY.

UNCLASSIFIED

SECURITY CLASSIFICATION OF THIS PAGE (When Data Entered)

REPORT DOCUMENTATION PAGE

READ INSTRUCTIONS BEFORE COMPLETING FORM

1. REPORT NUMBER (14) DTNSRDC-79/064	2. GOVT ACCESSION NO.	3. RECIPIENT'S CATALOG NUMBER
4. TITLE (and Subtitle) (6) DESIGN EQUATIONS FOR TRIPPING OF STIFFENERS UNDER INPLANE AND LATERAL LOADS		5. TYPE OF REPORT & PERIOD COVERED (9) Final rept.,
		6. PERFORMING ORG. REPORT NUMBER
7. AUTHOR(s) (10) John C./Adamchak		8. CONTRACT OR GRANT NUMBER(s)
9. PERFORMING ORGANIZATION NAME AND ADDRESS David W. Taylor Naval Ship Research and Development Center Bethesda, Maryland 20084		10. PROGRAM ELEMENT, PROJECT, TASK AREA & WORK UNIT NUMBERS (See reverse side)
11. CONTROLLING OFFICE NAME AND ADDRESS Naval Sea Systems Command Washington, D.C. 20362 (12) 99		12. REPORT DATE (11) Oct[redacted]1979
		13. NUMBER OF PAGES 99
14. MONITORING AGENCY NAME & ADDRESS(if different from Controlling Office) (16) F43422 (17) SF43422593		15. SECURITY CLASS. (of this report) UNCLASSIFIED
		15a. DECLASSIFICATION/DOWNGRADING SCHEDULE

16. DISTRIBUTION STATEMENT (of this Report)

APPROVED FOR PUBLIC RELEASE: DISTRIBUTION UNLIMITED

17. DISTRIBUTION STATEMENT (of the abstract entered in Block 20, if different from Report)

18. SUPPLEMENTARY NOTES

19. KEY WORDS (Continue on reverse side if necessary and identify by block number)

Lateral-Torsional Instability	Buckling Analysis
Tripping	Collapse Analysis
Stiffener Instability	

20. ABSTRACT (Continue on reverse side if necessary and identify by block number)

A series of design oriented equations to predict the tripping (lateral-torsional instability) of stiffeners under inplane and lateral loads has been developed which will allow this mode of failure to be more comprehensively addressed in the early stages of structural design. This type of failure is characterized by a twisting of the

(Continued on reverse side)

DD FORM 1 JAN 73 1473 EDITION OF 1 NOV 65 IS OBSOLETE
S/N 0102-LF-014-6601

UNCLASSIFIED

SECURITY CLASSIFICATION OF THIS PAGE (When Data Entered)

387 682

(Block 10)

Task Area SF 43 422 593
Program Element 62543N
Work Units 1730-593 and
1730-610

(Block 20 continued)

stiffener about its line of attachment to the plating and has been demonstrated by some recent British grillage tests to have serious potential as a primary mode of failure. The solutions developed take into account the effects of (1) the rotational resistance provided by the plating to which the stiffener is attached, (2) nonlinear material and structural behavior by means of a tangent modulus type approach, and (3) stiffener web deformations (for inplane loading). The equations are suitable for manual calculations but particularly powerful applications are possible when they are teamed up with a desk-top type mini-computer.

A number of comparisons between tripping predictions made using these equations and numerical finite element results in general show very good agreement. For the case of lateral loading the agreement is less consistently acceptable, primarily because of the more complicated nature of the tripping mode shapes and the inability at present to include the effects of web deformations for this loading. Comparisons are also made with experimental collapse data from two of the British grillages which failed by tripping and the agreement is quite good. Unfortunately, the mean tripping failure stresses (the basis of these comparisons) are quite sensitive to the estimates of plating effectiveness and thus wide variations in predicted mean stresses are possible. Thus, this limited experimental validation is not as conclusive as might be hoped for.

The development of these design equations is quite timely in view of the current interest being shown in the use of bulbs and flat bars as stiffening members (for reasons of economy). Such members are inherently weak with respect to tripping and their application would require that careful attention be given to tripping behavior.

Accession For
NTIS GRA&I ☑
DDC TAB ☐
Unannounced ☐
Justification
By
Distribution/
Availability Codes
Dist. A
Avail and/or special

TABLE OF CONTENTS

Page

LIST OF FIGURES iii

LIST OF TABLES iv

NOTATION vi

ABSTRACT 1

ADMINISTRATIVE INFORMATION 1

INTRODUCTION 2

TRIPPING UNDER AXIAL OR LATERAL LOADS 3
  TRIPPING UNDER END LOADS 8
  TRIPPING UNDER UNIFORM LATERAL LOADING 17
  COMPARISONS WITH NUMERICAL SOLUTIONS 23

EFFECTS OF WEB DEFORMATIONS 32

TRIPPING UNDER COMBINED LOADING 51

ESTIMATION OF PLATE ROTATIONAL RESTRAINT 55

INELASTIC EFFECTS 59

CONCLUSIONS 63

ACKNOWLEDGMENTS 66

APPENDIX A - SAMPLE PROBLEMS 67

APPENDIX B - QUADRATIC COEFFICIENTS FOR $H_m(K)$ AND $F_{in}(K)$ FUNCTIONS 79

APPENDIX C - COMPARISONS WITH EXPERIMENTAL DATA 83

REFERENCES 87

LIST OF FIGURES

1 - Characterization of Tripping 3

2 - Geometrical Tripping Parameters for Tee Stiffeners 6

Page

3 - Sign Convention for Inplane Axial and Shear Stress Components 8

4 - Geometry of External Loadings 9

5 - Distribution of Inplane Stress 13

6 - Stiffener Geometries for Comparative Solutions 24

7 - Characterization of Web Deformations 33

8 - Interaction Diagram for Combined Axial and Lateral Loads 53

LIST OF TABLES

1 - Tripping Stress Coefficients under End Loads and Moments (No Rotational Restraint) 25

2 - Tripping Load Coefficients under Uniform Lateral Load (No Rotational Restraint) 26

3 - Tripping Stress Coefficients for Flat Bars under End Loads and Moments with Rotational Restraint 28

4 - Tripping Stress Coefficients for Tees under End Loads and Moments with Rotational Restraint 29

5 - Tripping Load Coefficients under Uniform Lateral Load with Rotational Restraint 30

6 - Tripping Stress Coefficients for Tees under End Loads with Rotational Restraint 44

7 - Tripping Load Coefficients for Tees under End Moments with Rotational Restraint 45

8 - Tripping Stress Coefficients for Flat Bars under End Loads with Rotational Restraint 46

9 - Tripping Load Coefficients for Flat Bars under End Moments with Rotational Restraint 47

Page

10 - Tripping Stress Coefficients for Tees under End Loads with Varying Length/Depth Ratios (No Rotational Restraint) 49

11 - Tripping Stress Coefficients for Flat Bars under End Loads with Varying Length/Depth Ratios (No Rotational Restraint) 50

NOTATION

A_f	Cross-sectional area of stiffener flange
A_s	Cross-sectional area of stiffener
a	Length of stiffener between transverse supports
b	Uniform stiffener spacing
b_e	Plating effective width
C	Rotational spring constant (moment/length) of supporting plating
C_o	Rotational spring constant of unloaded supporting plating
c_j	Coefficients in thin plate theory tripping equation
D	Flexural rigidity of plating
D_w	Flexural rigidity of web plating of stiffener
d	Depth of flat bar stiffener; overall depth of tee stiffener
d_c	Depth of stiffener to midthickness of flange
d_w	Depth of stiffener web
E	Material Young's modulus
E_t	Material tangent modulus
$F_m(K)$	Quadratic function for tripping under lateral loading
f_w	Width of stiffener flange
f_0, f_1, f_2	Coefficients in $F_m(K)$ function
G	Material shear modulus
$H_m(K), \overline{H}_m(K)$	Quadratic functions for tripping under lateral loading

h	Height of neutral axis of plate-stiffener combination from midplane of plating
h_0, h_1, h_2	Coefficients in $H_m(K)$ function
$\bar{h}_0, \bar{h}_1, \bar{h}_2$	Coefficients in $\bar{H}_m(K)$ function
I	Effective vertical moment of inertia of stiffener and associated effective width of plating
I_p	Polar moment of inertia of stiffener about toe
I_{ps}	Polar moment of inertia of stiffener about shear center
I_t	Vertical moment of inertia of stiffener (alone) about toe
I_z	Moment of inertia of stiffener about web plane
I_{zf}	Moment of inertia of stiffener flange about web plane
J	St. Venant torsion constant for stiffener
K	Mode shape weighing factor
k_j	Coefficients in axial load tripping equation
$\bar{k}_j$	Coefficients in constant moment tripping equation
M	Vertical bending moment
M_{cre}, M_{cr}	Elastic, inelastic (vertical) tripping moments
M_p	Fully plastic moment of plate-stiffener cross section
m	Mode number
P	Axial end load
p_r	Structural proportional limit ratio
q	Uniform lateral loading (force/length)
q_{cre}, q_{cr}	Elastic, inelastic uniform lateral tripping load

R	Dimensionless rotational restraint parameter
R_c	Dimensionless rotational restraint coefficient
S	Plate-stiffener geometrical parameter
$\overline{s}$	Height of stiffener shear center above toe
t	Plate thickness
t_f	Stiffener flange thickness
t_w	Stiffener web thickness
U	Total potential energy of structure
U_w	Potential energy of the loading
V	Total strain energy of the structure
v	Sideways flexure of stiffener shear center*
v_o	Sideways flexure amplitude coefficient
$v_w(z)$	Sideways flexure of stiffener web midplane
W	Total work of applied forces
W_p	Work component of axial end load
W_q	Work component of uniform lateral loading
w	Vertical flexure of stiffener; lateral flexure of plate*
w_o	Plate lateral flexure amplitude coefficient
$\overline{z}$	Height of stiffener centroid above toe
α, β	Parameters in thin plate theory tripping equation
α, β, γ	Empirical indices in combined load tripping interaction formula

---

*Note: x and z subscripts applied to these parameters indicate partial derivatives with respect to those coordinates.

β	Rotation of stiffener shear center*
β_o	Rotation amplitude coefficient
Γ	Stiffener longitudinal warping constant
γ	Rotation of stiffener toe
δ	Stiffener axial shortening
ν	Material Poisson's ratio
σ_a	Average axial stress in plating (alone)
σ_e	Axial stress in stiffener
$(\sigma_e)_{cre}, (\sigma_e)_{cr}$	Elastic, inelastic axial tripping stress in stiffener
$(\sigma_e)^m_{pbe}$	Axial stress in stiffener at elastic plate buckling for mode m
$(\sigma_e)_{pbe}$	Axial stress in stiffener at minimum elastic plate buckling load
$(\sigma_m)_{cre}$, $(\sigma_m)_{cr}$	Elastic, inelastic mean axial tripping stress over the total plate-stiffener cross section
σ^m_{pbe}	Classical, elastic, uniform plate buckling stress for mode m
$\sigma_{pbe}, \sigma_{pb}$	Elastic, inelastic uniform plate buckling stress, minimum value
σ_{ps}	Structural proportional limit stress
$\sigma_x, \sigma_z, \tau_{xz}$	Inplane axial and shear stress components in stiffener web
σ_Y	Material tensile yield stress
Φ	Kernel of total potential energy integral

---

*Note: x and z subscripts applied to these parameters indicate partial derivatives with respect to those coordinates.

ABSTRACT

A series of design oriented equations to predict the tripping (lateral-torsional instability) of stiffeners under inplane and lateral loads has been developed which will allow this mode of failure to be more comprehensively addressed in the early stages of structural design. This type of failure is characterized by a twisting of the stiffener about its line of attachment to the plating and has been demonstrated by some recent British grillage tests to have serious potential as a primary mode of failure. The solutions developed take into account the effects of (1) the rotational resistance provided by the plating to which the stiffener is attached, (2) non-linear material and structural behavior by means of a tangent modulus type approach, and (3) stiffener web deformations (for inplane loading). The equations are suitable for manual calculations but particularly powerful applications are possible when they are teamed up with a desk-top type mini-computer.

A number of comparisons between tripping predictions made using these equations and numerical finite element results in general show very good agreement. For the case of lateral loading the agreement is less consistently acceptable, primarily because of the more complicated nature of the tripping mode shapes and the inability at present to include the effects of web deformations for this loading. Comparisons are also made with experimental collapse data from two of the British grillages which failed by tripping and the agreement is quite good. Unfortunately, the mean tripping failure stresses (the basis of these comparisons) are quite sensitive to the estimates of plating effectiveness and thus wide variations in predicted mean stresses are possible. Thus, this limited experimental validation is not as conclusive as might be hoped for.

The development of these design equations is quite timely in view of the current interest being shown in the use of bulbs and flat bars as stiffening members (for reasons of economy). Such members are inherently weak with respect to tripping and their application would require that careful attention be given to tripping behavior.

ADMINISTRATIVE INFORMATION

The work described in this report was performed at the David W. Taylor Naval Ship Research and Development Center under the sponsorship of the

NAVSEA 6.2 Exploratory Development Program, specifically the Surface Ship Structures Block, Program Element 62543N, Task Area SF 43 422 593 and Work Units 1730-593 and 1730-610.

INTRODUCTION

A series of tests on ship-type steel grillages conducted at the Naval Construction Research Establishment (NCRE) and recently reported[1*] has clearly demonstrated the significance of lateral-torsional instability (tripping) as a primary ductile failure mode for ship structure. The potential for such failure has important ramifications with regard to structural weight, fabrication cost, and structural reliability. Whereas tripping brackets, which are perhaps the most common measure employed to prevent this ailment, are advantageous from a weight standpoint, they suffer the disadvantages of increasing fabrication cost and of introducing hard spots at their toes which may give rise to fatigue problems and weaken the structure under explosive loading. In any case it seems clear that the ability to predict tripping failure in the early stages of design can have important consequences on the design of both conventional and high performance ships.

Surprisingly little material exists in the literature on the subject of tripping of stiffeners welded to continuous plating. In the elastic region tripping stresses can be estimated using approximate formulas[2,3] (for certain selected cases of loading) or more generally using folded-plate[4,5] or finite element analysis. In the inelastic region no satisfactory method appears to exist at present although the application of incremental finite element analysis would appear to offer great promise.

The main thrust of this study is the development of fast, approximate methods of tripping analysis for particular application in the concept, feasibility, and preliminary stages of design. As mentioned above, approximate formulas do exist in the literature, however, the work described herein both modifies and extends these previous efforts. As with these previous efforts, the solutions developed are elastic in nature; inelastic effects must be accounted for by modifying the elastic solutions, an admittedly crude approach. Nevertheless, the value of having relatively simple, approximate solutions at the early design stages (when more sophisticated solutions are often not practical) cannot be overstated; many of the most significant and critical decisions are made during these early design stages.

---

*A complete listing of references is given on page 87.

TRIPPING UNDER AXIAL OR LATERAL LOADS

Lateral-torsional, or tripping instability is characterized by a twisting of the stiffener about its line of attachment to the plating. This deformation pattern involves both sideways and vertical flexure (v,w) and rotation (β) of the stiffener as shown in Figure 1. If the centerline of

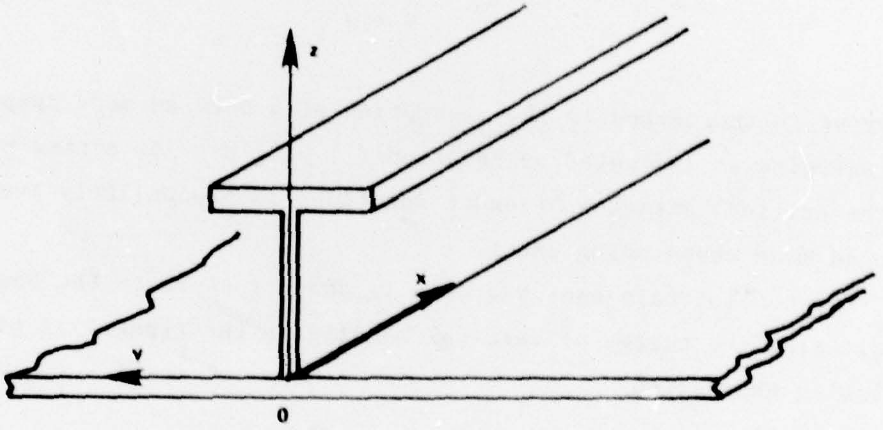

Figure 1a - Coordinate System

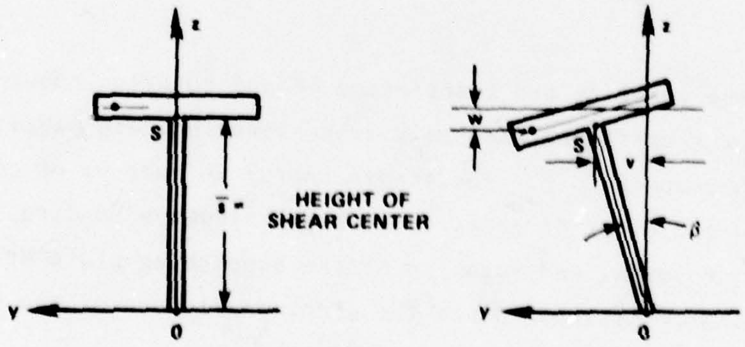

Figure 1b - Undeformed

Figure 1c - Deformed

Figure 1 - Characterization of Tripping

the web at any transverse cross section is not allowed to curve, then the three displacement degrees of freedom v, w, and β are coupled since, for small displacements, $v \approx z\beta$ and $w \approx -y\beta$.

The critical load for tripping is approximated by applying Rayleigh's principle. This principle states that for all possible deformations, the total strain energy V is greater than or equal to the work W done by the externally applied forces (or by the internal stress field arising from such forces). As a consequence, it is possible to obtain an approximate critical buckling stress, one that is always greater than the true buckling value, by equating the total strain energy and external work, i.e.,

$$V = W \tag{1}$$

Inherent in the method is the assumption of a buckled mode shape; equating the energies as indicated by Equation (1) will provide either upper bounds to the critical stresses or exact solutions in the unlikely event of the assumed mode shape being exact.

The total strain energy stored in the structure in the buckled state (neglecting the energy of vertical bending in the flange) is given by the following expression

$$V = \frac{1}{2} \int_0^a [EI_z \, v_{xx}^2 + E\Gamma \, \beta_{xx}^2 + GJ \, \beta_x^2 + C\beta^2] \, dx \tag{2}$$

where v and β here refer to the translation of and rotation about the shear center of the stiffener and the x subscripts indicate partial derivatives with respect to x. The strain energy is made up of contributions from (in the order of appearance above) sideways bending, longitudinal warping, torsion, and rotation of the supporting plate structure modeled as an elastic spring. Since the sideways flexure of the shear center is coupled to the rotation β as indicated,

$$v \approx \bar{s}\beta \tag{3}$$

the sideways bending and longitudinal warping terms can be combined to give

$$V = \frac{1}{2} \int_0^a \left[E(I_z \bar{s}^2 + \Gamma)\, \beta_{xx}^2 + GJ\, \beta_x^2 + C\beta^2\right] dx \tag{4}$$

In this expression a is the length of the stiffener between transverse supports, E and G are the Young's and shear moduli of the material, respectively, and C is the rotational spring constant (per unit length) of the supporting structure. The coefficients I_z, $\bar{s}$, Γ, and J are defined in Figure 2 in terms of the geometry of the stiffener.

Although Equation (4) may be applied to flat bars as well as flanged stiffeners, it is perhaps more appropriate for thin flat bars to use the expression for strain energy derived from thin plate theory, namely

$$V = \frac{1}{2} D_w \int_0^a \int_0^{d(x)} \{(v_{xx}+v_{zz})^2 - 2(1-\nu)\,[v_{xx}\, v_{zz} - v_{xz}^2]\}\, dxdz$$

$$+ \frac{1}{2} \int_0^a C\beta^2\, dx \tag{5}$$

where D_w is the well known plate flexural rigidity (for the flat bar), ν is Poisson's ratio, and d(x) represents the depth of the flat bar at location x.

In computing the work W the nature of the external loading will often dictate the form of the expressions used. When axial end thrusts and/or moments are applied at the stiffener ends it is usually most convenient to

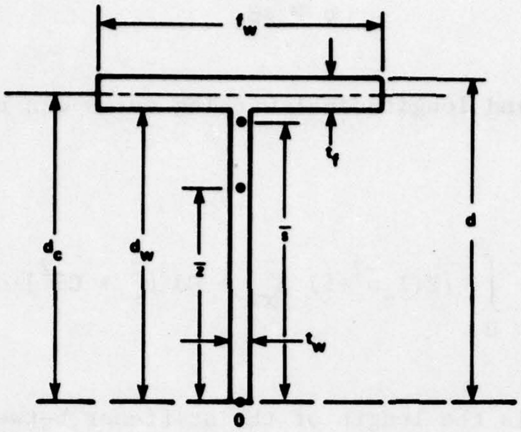

I_z - Moment of Inertia about the Web Plane

$$I_z = \frac{1}{12}\left(t_f f_w^3 + d_w t_w^3\right)$$

$\bar{s}$ - Height of Shear Center above Toe (Origin)

$$\bar{s} = \frac{1}{2}\left[d_w + \frac{d_w + t_f}{1 + (d_w/t_f)(t_w/f_w)^3}\right] \approx d_c$$

Γ - Longitudinal Warping Constant

$$\Gamma = \frac{1}{36}\left(t_w^3 d_w^3 + \frac{1}{4} t_f^3 f_w^3\right)$$

J - St. Venant Torsion Constant

$$J = \frac{1}{3}\left(d_w t_w^3 + f_w t_f^3\right)$$

I_t - Vertical Moment of Inertia about Toe (Stiffener alone)

$$I_t = \frac{1}{3} t_w d_w^3 + f_w t_f \left(d_c^2 + \frac{1}{12} t_f^2\right)$$

I_p - Polar Moment of Inertia about Toe

$$I_p = I_t + I_z$$

$\bar{z}$ - Height of Centroid above Toe

$$\bar{z} = \left[\frac{1}{2} t_w d_w^2 + f_w t_f d_c\right] \Big/ \left[t_w d_w + f_w t_f\right]$$

Figure 2 - Geometrical Tripping Parameters for Tee Stiffeners

compute the component of work done by these forces by integrating the product of the axial stresses arising from these forces and the axial shortening $\delta(y,z)$ of the stiffener at the point in question, namely,

$$W = \iint \sigma_x \, \delta(y,z) \, dydz \tag{6}$$

As the expression suggests, the integration is carried out over the area of the stiffener end. When the stiffener has lateral loading the above approach cannot be applied, rather the work done by the internal stress field arising from the lateral loading is computed according to

$$W = \frac{1}{2} \int_0^a \int_0^{d_w(x)} [\sigma_x (v_x)^2 + \sigma_z (v_z)^2 - 2 \, \tau_{xz} \, v_x \, v_z] \, t_w \, dzdx$$

$$+ \frac{1}{2} \int_0^a [\sigma_x (v_x^2 + w_x^2)]_{z=d_c} \, f_w t_f dx \tag{7}$$

where the first integral represents the action of the stress field in the web and the second that in the flange. When both lateral and end loadings are present, the stress fields arising from each set of loads may be separated and the corresponding work components computed according to Equations (6) and (7), as appropriate.

The signs of the terms in Equation (7) differ in some respects from those found in other references. This is due to the assumption of compression as a positive stress and tension as negative. (This is quite common in compression instability work.) Figure 3 defines the sign convention adopted in this report for the σ_x, σ_z, and τ_{xz} stresses and the corresponding equilibrium equations which are consistent with Equation (7).

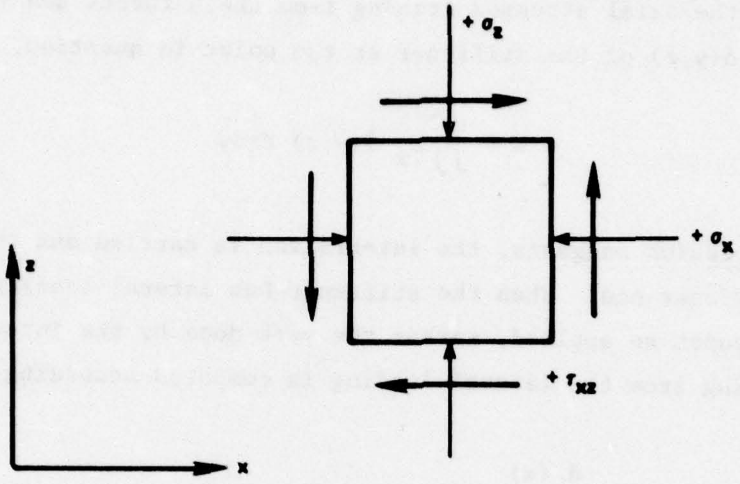

EQUILIBRIUM EQUATIONS

$$\frac{\partial \sigma_x}{\partial x} - \frac{\partial \tau_{xz}}{\partial z} = 0$$

$$\frac{\partial \sigma_z}{\partial z} - \frac{\partial \tau_{xz}}{\partial x} = 0$$

Figure 3 - Sign Convention for Inplane Axial and Shear Stress Components

TRIPPING UNDER END LOADS

Consider a single stiffener of constant cross section and its associated frame space of plating loaded by an axial inplane force of magnitude P as shown in Figure 4. The ends of the stiffener will experience a uniform axial stress σ_e which is related to the cross sectional area of the stiffener A_s, the plating thickness t, and the plating effective width b_e, as follows,

$$\sigma_e = \frac{P}{A_s + b_e t} \tag{8}$$

In terms of the stress components in the stiffener, σ_x, σ_z, and τ_{xz}, this translates into

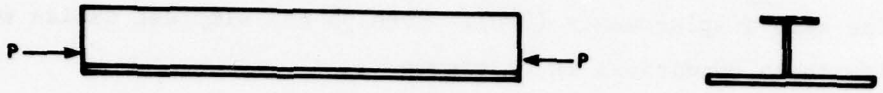

Figure 4a - Axial Force

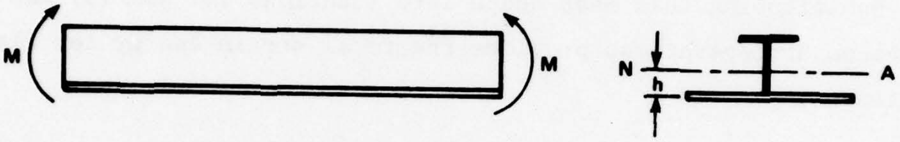

Figure 4b - Constant Moment

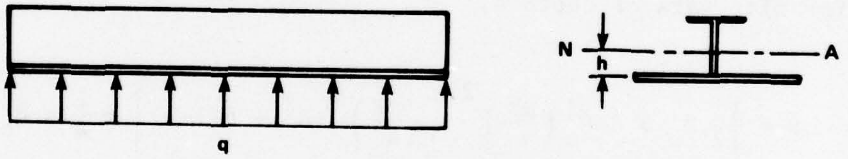

Figure 4c - Uniform Lateral Load

Figure 4 - Geometry of External Loadings

$$\sigma_x = \sigma_e \tag{9}$$

$$\sigma_z = 0 \tag{10}$$

$$\tau_{xz} = 0 \tag{11}$$

To calculate the strain energy in the stiffener and the work done by the axial load, an assumption has to be made for the buckled mode shape. Because of the repeatability and continuity of typical ship structure, it is logical to select a mode shape incorporating simply supported boundaries, ($\beta_{xx}=0$) at the ends $x = 0$ and $x = a$ in addition to the requirements for zero displacements ($\beta=0$). Perhaps the simplest choice which satisfies these conditions is to assume

$$\beta = \beta_o \sin \frac{m\pi x}{a} \tag{12}$$

Substituting this mode shape into Equations (4) and (5) and performing the necessary operations provides the total strain energy for flanged stiffeners,

$$V = \frac{1}{4} a \beta_o^2 \left[E(I_z \bar{s}^2 + \Gamma) \left(\frac{m\pi}{a}\right)^4 + GJ \left(\frac{m\pi}{a}\right)^2 + C \right] \tag{13}$$

and for flat bars of depth d,

$$V = \frac{1}{12} D_w a d \beta_o^2 \left(\frac{m\pi}{a}\right)^2 \left[\left(\frac{m\pi}{a}\right)^2 d^2 + 6(1-\nu) \right] + \frac{1}{4} a \beta_o^2 C \tag{14}$$

The work done by the axial inplane force is computed according to Equation (6). The relative displacement of the two ends of the stiffener δ due to its curvature for a fiber at location (y,z) is given by

$$\delta(y,z) = \frac{1}{2} \int_0^a [v_x^2 + w_x^2]\, dx \tag{15}$$

Since $v \approx z\beta$ and $w \approx -y\beta$, this expression transforms to

$$\delta(y,z) = \frac{1}{2} \int_0^a [z^2 + y^2]\, \beta_x^2\, dx \tag{16}$$

which, in turn, upon substitution of Equation (12) becomes

$$\delta(y,z) = \frac{1}{4}\,[z^2 + y^2]\,\beta_o^2\left(\frac{m\pi}{a}\right)^2 a \qquad (17)$$

The work, therefore, is

$$W = \sigma_e \cdot \frac{1}{4}\,\beta_o^2\left(\frac{m\pi}{a}\right)^2 a \iint_{A_s} [z^2 + y^2]\,dydz \qquad (18)$$

where the integration over the stiffener cross section is carried out at the point of load application. Since

$$\iint_{A_s} [z^2 + y^2]\,dydz = I_p \qquad (19)$$

(see Figure 2) the expression for the work of the external force may be further transformed,

$$W = \frac{1}{4}\,\sigma_e\,\beta_o^2\left(\frac{m\pi}{a}\right)^2 a\,I_p \qquad (20)$$

Equating the total strain energy and the work leads to the critical elastic value of stress for stiffener tripping. For flanged stiffeners this stress is

$$(\sigma_e)_{cre} = \left(\frac{1}{I_p}\right)\left[GJ + E(I_z\bar{s}^2+\Gamma)\left(\frac{m\pi}{a}\right)^2 + C\left(\frac{a}{m\pi}\right)^2\right] \qquad (21)$$

and for flat bars,

$$(\sigma_e)_{cre} = \frac{1}{3}\frac{D_w d}{I_p}\left[\left(\frac{m\pi}{a}\right)^2 d^2 + 6(1-\nu)\right] + \frac{C}{I_p}\left(\frac{a}{m\pi}\right)^2 \tag{22}$$

where (for flat bars)

$$I_p = \frac{1}{3} t_w d^3 + \frac{1}{12} d t_w^3 \approx \frac{1}{3} t_w d^3 \tag{23}$$

In actual fact these solutions are exact, as comparisons with published solutions[6] will demonstrate. (This is of course subject to the condition stated earlier of zero curvature v_{zz} of the stiffener web.) Thus, Equation (12) in this case represents the exact tripping mode shape.

When there is no restraint against rotation, $C = 0$, it can be seen by inspection that the lowest buckling stress occurs for one wave, $m = 1$. When C is nonzero, the mode number for which $(\sigma_e)_{cre}$ is lowest is dependent on the degree of restraint. Although m takes on only integer values, the determination of the critical stress can be simplified by setting

$$\frac{\partial(\sigma_e)_{cre}}{\partial m} = 0 \tag{24}$$

solving for m, and then comparing the tripping stresses for the two integer values of m which bracket this value. From the above conditions one obtains

$$m = \frac{a}{\pi}\left[\frac{C}{E(I_z \bar{s}^2 + \Gamma)}\right]^{1/4} \tag{25}$$

for flanged stiffeners, and

$$m = \frac{a}{\pi}\left[\frac{3C}{D_w d^3}\right]^{1/4} \tag{26}$$

for flat bars.

It is important to note here that the stress $(\sigma_e)_{cre}$ is a peak stress at the stiffener location and that when the effective width of the plating b_e is less than b this stress will be greater than both the corresponding average stress in the plating σ_a and the mean stress over the total plate-beam cross section, σ_m. These definitions of stress are illustrated in Figure 5. Since the mean stress is frequently used in design calculations

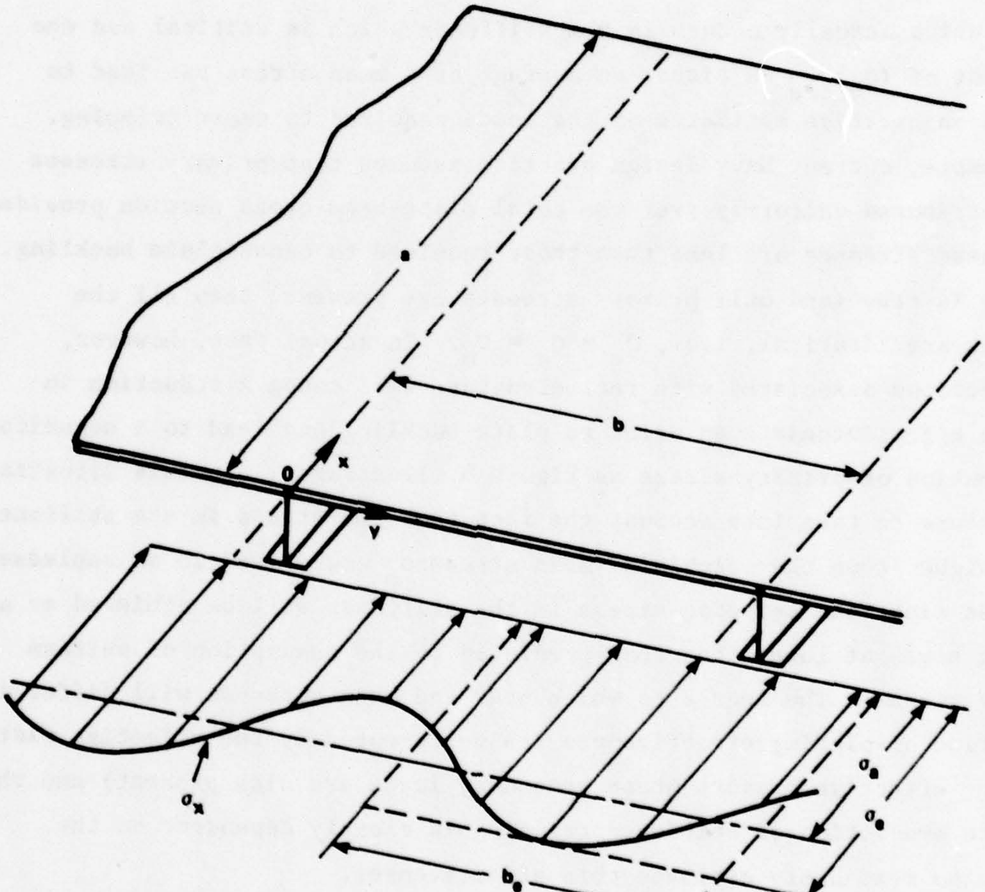

AVERAGE PLATE STRESS $\sigma_a = \frac{b_e}{b} \sigma_e$

MEAN STRESS $\sigma_m = \left(\frac{A_s + b_e t}{A_s + bt}\right) \sigma_e$

Figure 5 - Distribution of Inplane Stress

the peak stresses given by Equations (21) and (22) can readily be converted to the mean form according to

$$(\sigma_m)_{cre} = \left(\frac{A_s+b_et}{A_s+bt}\right)(\sigma_e)_{cre} \tag{27}$$

The distinction between peak, average (plate), and mean stresses is a particularly significant point with regard to tripping since it is the stress which actually occurs in the stiffener which is critical and the treatment of $(\sigma_e)_{cre}$ as either an average or a mean stress can lead to very unconservative estimates of the loads required to cause tripping. For example, current Navy design practice assumes that primary stresses are distributed uniformly over the total plate-beam cross section provided that these stresses are less than those required to cause plate buckling. If this is true (and only primary stresses are present) then all the stresses are identical, i.e., $\sigma_e = \sigma_a = \sigma_m$. In actual fact, however, imperfections associated with real structure will cause a reduction in plating effectiveness even prior to plate buckling and lead to a nonuniform distribution of primary stress as Figure 5 illustrates. In this situation the failure to take into account the fact that the stress in the stiffener σ_e is higher than the calculated mean stress σ_m could lead to an unpleasant surprise since the tripping stress in the stiffener will be achieved at a loading somewhat lower than that predicted by the assumption of uniform primary stress. The degree to which peak and mean stresses will differ is a function of plating effectiveness, as represented by the effective width (and the effective breadth where secondary loads are also present) and the accurate prediction of stiffener tripping is clearly dependent on the ability to reasonably estimate this effectiveness.

If the plate-stiffener combination is loaded by a constant moment M, as shown in Figure 4b, the stress distribution will no longer be constant over the cross section but rather will vary linearly from plate to flange. Thus in terms of σ_x, σ_z, and τ_{xz} one obtains

$$\sigma_x = \left(\frac{M}{I}\right)\left(z-h+\frac{1}{2}t\right) \tag{28}$$

$$\sigma_z = 0 \tag{29}$$

$$\tau_{xz} = 0 \tag{30}$$

where I is the vertical moment of inertia of the stiffener and its associated effective breadth of plating and h is the corresponding location of the neutral axis from the midplane of the plating.

If the same mode shape, Equation (12), is assumed, then the expressions for total strain energy are once again given by Equations (13) and (14). The work is computed using Equations (6) and (17) leading to

$$W = \frac{1}{4} \beta_o^2 \left(\frac{m\pi}{a}\right)^2 a \left(\frac{M}{I}\right) \iint_{A_s} [z^2 + y^2] \left[z - h + \frac{1}{2} t\right] dydz \tag{31}$$

The integral in this expression is broken up into two parts, one for the web and one for the flange

$$\iint_{A_s} [z^2 + y^2] \left[z - h + \frac{1}{2} t\right] dydz$$

$$= \int_0^{d_w} \int_{-\frac{1}{2} t_w}^{+\frac{1}{2} t_w} [z^2 + y^2] \left[z - h + \frac{1}{2} t\right] dydz$$

$$+ \int_{d_w}^{d} \int_{-\frac{1}{2} f_w}^{+\frac{1}{2} f_w} [z^2 + y^2] \left[z - h + \frac{1}{2} t\right] dydz \tag{32}$$

Because the web depth and flange width are typically much larger than the web and flange thicknesses, these integrals can be simplified by making certain approximations, resulting in

$$\iint_{A_s} [z^2 + y^2] \left[z - h + \frac{1}{2} t\right] dydz$$

$$\approx - \left(h - \frac{1}{2} t\right) \iint_{A_s} (z^2+y^2)\, dydz$$

$$+ \int_0^{d_w} z^3\, t_w\, dz + \int_{-\frac{1}{2} f_w}^{+\frac{1}{2} f_w} d_c (d_c^2+y^2)\, t_f dy$$

$$= - \left(h- \frac{1}{2} t\right) I_p + \frac{1}{4} t_w d_w^4 + d_c \left(d_c^2 t_f f_w + \frac{1}{12} f_w^3 t_f\right)$$

$$= \frac{1}{4} \left[t_w d_w^4 - 4 \left(h - \frac{1}{2} t\right) I_p + 4\, d_c (A_f d_c^2+I_{zf})\right] \equiv S \qquad (33)$$

where I_{zf} and A_f are the moment of inertia about the web plane and the cross sectional area of the stiffener flange alone, respectively. Because this geometrical parameter will continually reappear in the later sections of this report it has been denoted by the symbol S as indicated above. The above expression is valid for both flanged stiffeners and flat bars although for flat bars the last term is obviously zero since both A_f and I_{zf} are identically zero.

Making use of this definition, the work done by the applied moment is given by

$$W = \frac{1}{4} \beta_o^2 \left(\frac{m\pi}{a}\right)^2 a \left(\frac{M}{I}\right) S \qquad (34)$$

As with the case of a concentrated force, the critical moment for elastic tripping is determined by equating the total strain energy and the work. The resulting expressions are

$$M_{cre} = \left(\frac{I}{S}\right) \left[E(I_z \bar{s}^2 + \Gamma) \left(\frac{m\pi}{a}\right)^2 + GJ + \left(\frac{a}{m\pi}\right)^2 C\right] \qquad (35)$$

for flanged stiffeners, and

$$M_{cre} = \left(\frac{I}{S}\right) \left[\frac{1}{3} D_w d \left\{\left(\frac{m\pi}{a}\right)^2 d^2 + 6(1-\nu)\right\} + \left(\frac{a}{m\pi}\right)^2 C\right] \qquad (36)$$

for flat bars.

For the case of no restraint against rotation (C=0) the critical moment also occurs for the mode shape corresponding to m = 1. When restraint does exist, the critical moment may be found using the same procedure as that described for constant force loading, and in fact, it is quite easy to show that the values of m, for which M_{cre} is minimum, are given by the identical expressions, Equations (25) and (26). It is also noteworthy that, for all practical considerations, only positive moments will cause tripping as indicated by Equations (35) and (36). Only when the neutral axis is located at a significant distance from the plating may a negative moment be likely to cause tripping and, in this case, the assumed deformation used in the preceding development would probably not be appropriate.

TRIPPING UNDER UNIFORM LATERAL LOADING

Many stiffened plate components of a ship routinely experience lateral loadings such that the possibility of tripping collapse due to such loadings (or at least in conjunction with inplane loading) is a definite possibility. If this type of failure is to be avoided, it is clear that the ability to predict tripping behavior under lateral loading is necessary. Since in many design calculations lateral loadings are idealized as uniformly distributed, the development which follows assumes such a distribution. However, the technique employed is not restricted to uniform distributions and can readily be applied to others as the need arises.

The critical lateral load for stiffener tripping is computed in the same manner as that for concentrated end loading, that is, the strain energy V is equated with the external work W for an assumed displacement function. In this case, however, W must be determined by computing the work done by the internal stress field arising from the presence of the lateral loading as indicated in Equation (7).

For a single stiffener and its associated frame spacing of plating, simply supported at its ends, the stress components due to a uniform lateral loading q, (positive in the positive z direction) are as follows,

$$\sigma_x = \frac{1}{2}\left(\frac{q}{I}\right)\left(z-h+\frac{1}{2}t\right)\left(x^2-ax\right) \tag{37}$$

$$\sigma_z = \left(\frac{q}{t_w}\right)-\left(\frac{q}{I}\right)\left[\frac{A_f z}{t_w}\left(d_c-h+\frac{1}{2}t\right) + z\left\{\frac{1}{2}d_w^2-\frac{1}{6}z^2+\left(h-\frac{1}{2}t\right)\left(\frac{1}{2}z-d_w\right)\right\}\right] \tag{38}$$

$$\tau_{xz} = \frac{1}{2}\left(\frac{q}{I}\right)(a-2x)\left[\frac{A_f}{t_w}\left(d_c-h+\frac{1}{2}t\right) + \frac{1}{2}d_w^2-\frac{1}{2}z^2+\left(h-\frac{1}{2}t\right)(z-d_w)\right] \tag{39}$$

(These stresses can readily be shown to satisfy the equilibrium equations given in Figure 3.)

Although it would appear logical to again adopt Equation (12) as the assumed displacement function, experience has indicated that due to the concentration of high σ_x stresses around the midlength of the stiffener this function is in serious error with respect to the true buckled state. An improved displacement function can be constructed by including a component of the next higher mode along with the primary mode, specifically,

$$\beta = \beta_o \left[K \sin \frac{m\pi x}{a} + (K-1) \sin \frac{(m+2)\pi x}{a} \right] \tag{40}$$

where m is the primary mode number. This expression incorporates an unknown coefficient K, which, in general, may take on values between approximately 1.5 and 0. Since the application of Rayleigh's principle produces a buckling load which is always greater than the true value, the appropriate value of K is selected by minimizing the value of the buckling load with respect to K.

The strain energy expressions are determined by substituting Equation (40) into Equations (4) and (5) and performing the necessary operations. This leads to

$$V = \frac{1}{4}\, a\, \beta_o^2 \left(\frac{\pi}{a}\right)^2 GJ\, H_m(K) \tag{41}$$

for flanged stiffeners, and

$$V = \frac{1}{12}\, D_w\, ad\, \beta_o^2 \left(\frac{\pi}{a}\right)^2 \overline{H}_m(K) \tag{42}$$

for flat bars. In these expressions $H_m(K)$ and $\overline{H}_m(K)$ are shorthand notation for quadratic functions in K which are defined as follows:

$$H_m(K) = \Big[\{m^2K^2 + (m+2)^2 (K-1)^2\} + \{m^4K^2$$

$$+ (m+2)^4 (K-1)^2\} \left(\frac{\pi}{a}\right)^2 \left(\frac{E}{GJ}\right) (I_z \bar{s}^{-2} + \Gamma)$$

$$+ \{K^2 + (K-1)^2\} \left(\frac{a}{\pi}\right)^2 \frac{C}{GJ} \Big] \tag{43a}$$

$$\bar{H}_m(K) = \Big[\left(\frac{\pi d}{a}\right)^2 \{m^4K^2 + (m+2)^4 (K-1)^2\}$$

$$+ 6(1-\nu) \{m^2K^2 + (m+2)^2 (K-1)^2\}$$

$$+ \frac{3C}{D_w d} \left(\frac{a}{\pi}\right)^2 \{K^2 + (K-1)^2\} \Big] \tag{43b}$$

The work W done by the internal stress field is calculated using Equation (7), giving

$$W = - \frac{1}{48} \left(\frac{q}{I}\right) \beta_o^2 \pi^2 a S F_m(K) \tag{44}$$

where once again, for reasons of convenience, shorthand notation is used to represent a quadratic function in K, namely

$$F_m(K) = m^2 K^2 \left(1 - \frac{3}{m^2\pi^2}\right) + \frac{6m}{\pi^2} (m+2) \Big\{ 1$$

$$+ \frac{1}{(m+1)^2} \Big\} K(1-K) + (m+2)^2 (K-1)^2 \Big\{ 1$$

$$- \frac{3}{\pi^2 (m+2)^2} \Big\} - \frac{6d_w}{\pi^2 S} \left[A_f t_f \left(d_c - h + \frac{1}{2} t\right) + b_e t^2 h \right] [K^2$$

$$+ (K-1)^2] \tag{45}$$

Equating the strain energy and the work, and then solving for q results in the critical value of the lateral loading. For flanged stiffeners one gets

$$q_{cre} = -\frac{12IGJ}{Sa^2} \cdot \frac{H_m(K)}{F_m(K)} \tag{46}$$

and in a similar fashion for flat bars,

$$q_{cre} = -\frac{4IdD_w}{Sa^2} \cdot \frac{\overline{H}_m(K)}{F_m(K)} \tag{47}$$

The above expressions for q_{cre} contain the parameter K whose value at this point is still unknown. As previously mentioned the appropriate value of K is determined by minimizing the value of q_{cre} with respect to K. This process is routinely carried out by setting the derivative, $\partial q_{cre}/\partial K = 0$ and solving for K.

In the above expressions for q_{cre}, the K terms only appear in the $H_m(K)/F_m(K)$ and $\overline{H}_m(K)/F_m(K)$ ratios. Since the H's and F's are quadratic functions, they can symbolically be represented in the form

$$H_m(K) = h_0 + h_1K + h_2K^2 \tag{48a}$$

$$F_m(K) = f_0 + f_1K + f_2K^2 \tag{48b}$$

It can readily be shown that setting the derivative $\partial q_{cre}/\partial K$ equal to zero leads to a third quadratic equation in K,

$$[h_1f_2 - h_2f_1]K^2 + 2[h_0f_2 - h_2f_0]K + [h_0f_1 - h_1f_0] = 0 \tag{49}$$

the solution of which provides the value of K for which $H_m(K)/F_m(K)$, and hence, q_{cre}, is a minimum. The above equation being quadratic, usually two distinct values of K will result. The appropriate choice of K, however, is usually quite obvious as is discussed later in Appendix A in connection with the illustrative examples.

The expressions for $H_m(K)$, $\overline{H}_m(K)$, and $F_m(K)$ as given by Equations (43) and (45) are not in the form required for the determination of K according to the method represented by Equation (49). These expressions have been rearranged, however, and the forms most appropriate for use with Equation (49) are presented in Appendix B.

If the ends of the stiffener and its associated frame space of plating are clamped rather than simply-supported, the stress components due to a uniform lateral loading q are as follows,

$$\sigma_x = \frac{1}{2}\left(\frac{q}{I}\right)(x^2-ax)\left(z-h+\frac{1}{2}t\right) + \frac{1}{12}\left(\frac{q}{I}\right)a^2\left(z-h+\frac{1}{2}t\right) \tag{50}$$

$$\sigma_z = \left(\frac{q}{t_w}\right) - \left(\frac{q}{I}\right)\left[\frac{A_f z}{t_w}\left(d_c-h+\frac{1}{2}t\right) + z\left\{\frac{1}{2}d_w^2 - \frac{1}{6}z^2 + \left(h-\frac{1}{2}t\right)\left(\frac{1}{2}z-d_w\right)\right\}\right] \tag{51}$$

$$\tau_{xz} = \frac{1}{2}\left(\frac{q}{I}\right)(a-2x)\left[\frac{A_f}{t_w}\left(d_c-h+\frac{1}{2}t\right) + \frac{1}{2}d_w^2 - \frac{1}{2}z^2 + \left(h-\frac{1}{2}t\right)(z-d_w)\right] \tag{52}$$

If Equation (40) is again selected as the assumed displacement function, then the strain energy expressions are the same as for the simply supported case, namely Equations (41) and (42). The expressions for the external work, however, will not be identical since the σ_x stress component is different. The differences are entirely within the definition of the function $F_m(K)$, however, so that Equation (44) is valid for the clamped condition with $F_m(K)$ now defined as

$$F_m(K) = -\frac{3}{\pi^2} K^2 + \frac{6m}{\pi^2} (m+2) \left\{1 + \frac{1}{(m+1)^2}\right\} K(1-K) - \frac{3}{\pi^2} (K-1)^2$$

$$- \frac{6d_w}{\pi^2 S} \left[A_f t_f \left(d_c - h + \frac{1}{2} t\right) + b_e t^2 h\right] [K^2 + (K-1)^2] \qquad (53)$$

Using this definition of $F_m(K)$ the critical value q_{cre} may be computed using Equations (46) and (47) and the procedure previously outlined to determine the appropriate value of the parameter K. The expressions for the "clamped" version of $F_m(K)$ in the format which is symbolically represented by Equations (48) is also provided in Appendix B.

COMPARISONS WITH NUMERICAL SOLUTIONS

To demonstrate the application of these solutions and to shed some light on their approximate ranges of validity, several comparisons were made with solutions obtained by the finite element method, specifically with a program developed and documented at the University of California.[7] Both a flat bar and a tee stiffener configuration were considered, the proportions of which are provided in Figure 6.

Because of the symmetry of the structure and its response, it was necessary to model only one-half of each stiffener for the finite element analyses. A uniform mesh consisting of 10 rectangular plate elements in the x-direction and 8 elements in the z-direction was employed. The flange of the tee stiffener was modeled by an additional 10 bar-type elements. Although assumptions inherent to the finite element method mean that solutions obtained using the method are themselves approximate, the moderately fine mesh employed here can be expected to produce results which are at most a few percent different from the so-called theoretically "exact" values.

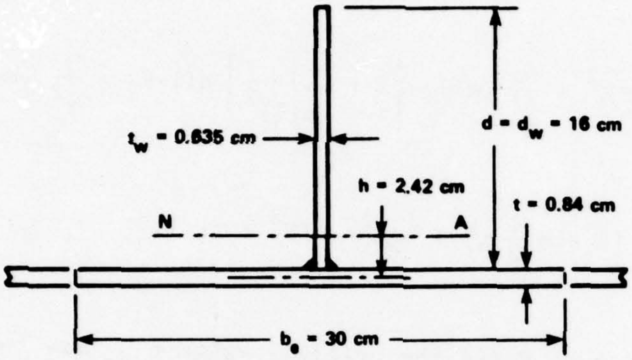
t_w = 0.635 cm
d = d_w = 16 cm
h = 2.42 cm
t = 0.84 cm
N
A
b_e = 30 cm

FLAT BAR STIFFENER – a = 100 cm

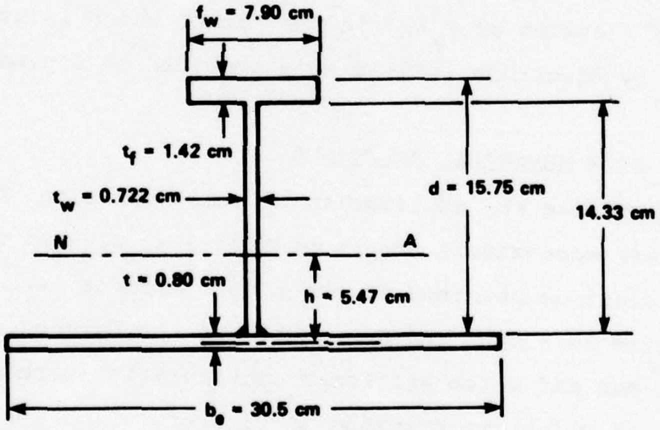
f_w = 7.90 cm
t_f = 1.42 cm
t_w = 0.722 cm
d = 15.75 cm
14.33 cm
N
A
t = 0.80 cm
h = 5.47 cm
b_e = 30.5 cm

TEE STIFFENER – a = 160 cm

Figure 6 - Stiffener Geometries for Comparative Solutions

Tables 1 and 2 provide buckling stress, moment, and lateral load coefficients for the first two modes for the case of zero rotational restraint at the stiffener base, i.e., C = 0. For the cases of axial end load and end moment agreement is, in general, very good between the finite element and energy solutions. For lateral loading, the agreement between the two methods of solution varies from very good to very poor, with the

TABLE 1 - TRIPPING STRESS COEFFICIENTS UNDER END LOADS AND MOMENTS (NO ROTATIONAL RESTRAINT)

Flat Bar		
Mode m	Tripping Stress Coefficient $[(\sigma_e)_{cre}/E] \times 10^4$	
	Finite Element	Eqn. (22)
1	6.44	6.42
2	7.58	7.51
Mode m	Tripping Moment Coefficient $\left[M_{cre}\left(d-h+\frac{1}{2}t\right) \times 10^4\right] / [IE]$	
	Finite Element	Eqn. (36)
1	9.04	8.99
2	10.66	10.52

Tee Stiffener		
Mode m	Tripping Stress Coefficient $[(\sigma_e)_{cre}/E] \times 10^4$	
	Finite Element	Eqn. (21)
1	26.4	26.3
2	65.9	72.6
Mode m	Tripping Moment Coefficient $\left[M_{cre}\left(d_c-h+\frac{1}{2}t\right) \times 10^4\right] / [IE]$	
	Finite Element	Eqn. (35)
1	29.4	29.0
2	75.1	80.1

TABLE 2 - TRIPPING LOAD COEFFICIENTS UNDER UNIFORM LATERAL LOAD (NO ROTATIONAL RESTRAINT)

Flat Bar			
Mode m	B.C.*	Tripping Load Coefficient $100\, q_{cre} \frac{a^2\left(d-h+\frac{1}{2}t\right)}{EI}$	
		Finite Element	Eqn. (47)
1	SS	- 1.13	- 1.12
2	SS	- 1.20	- 1.18
1	C	+ 1.76	+ 1.96
2	C	+ 3.18	+ 3.90
Tee Stiffener			
Mode m	B.C.*	Tripping Load Coefficient $100\, q_{cre} \frac{a^2\left(d_c-h+\frac{1}{2}t\right)}{EI}$	
		Finite Element	Eqn. (46)
1	SS	- 4.59	- 5.20
2	SS	- 9.03	-10.09
1	C	+ 6.54	+ 7.91
2	C	+17.91	+40.76

*B.C. = Boundary Conditions, SS = Simple Support, C = Clamped.

flat bar simply supported showing the best agreement and the clamped tee stiffener the worst. If restraint is added along the base of the stiffeners the discrepancies between the two methods consistently grow as the amount of the restraint is increased. This trend is clearly illustrated in Tables 3, 4, and 5 where buckling coefficients are tabulated as a function of a dimensionless restraint coefficient R_c, defined as

$$R_c = \frac{C\left(\frac{a}{m\pi}\right)^2}{GJ + E(I_z\bar{s}^2+\Gamma)\left(\frac{m\pi}{a}\right)^2} \tag{54}$$

for flanged stiffeners, and

$$R_c = \frac{C\left(\frac{a}{m\pi}\right)^2}{\frac{1}{3}\, D_w d\left[\left(\frac{m\pi}{a}\right)^2 d^2 + 6(1-\nu)\right]} \tag{55}$$

for flat bars.

If the finite element data is examined in more detail it becomes quite apparent that the primary cause of the discrepancies noted above is the presence of web deformations. To prevent overly optimistic buckling predictions, Faulkner in his work[3] suggested an upper limit on the value of C used as follows,

$$\frac{Ca^2}{\pi^2\, GJ} \leq 10 \tag{56}$$

For the tee stiffener cited here, however, this corresponds approximately to a value of $R_c = 4.1$ (for m=1) and from the data presented in the tables, the above limit itself would appear to be overly optimistic.

While the lack of consideration of web deformations appears to be the primary cause of the discrepancies noted in the tables, a possibly

TABLE 3 - TRIPPING STRESS COEFFICIENTS FOR FLAT BARS UNDER END LOADS AND MOMENTS WITH ROTATIONAL RESTRAINT

Flat Bar			
Mode m	R_c	Tripping Stress $[(\sigma_e)_{cre} \times 10^4]/E$ Coefficient	
		Finite Element	Eqn. (22)
1	0	6.44	6.42
2	0	7.58	7.51
3	0	--	9.33
1	2.0	17.6	19.3
2	0.427	10.5	10.7
3	0.153	10.9	10.8
1	10.0	41.2	70.6
2	2.14	16.9	23.6
3	0.764	14.1	16.5
Mode m	R_c	Tripping Moment Coefficient $\left[M_{cre}\left(d-h+\frac{1}{2}t\right) \times 10^4\right] / [IE]$	
		Finite Element	Eqn. (36)
1	0	9.04	8.99
2	0	10.66	10.52
1	2.0	24.3	27.0
2	0.427	14.6	15.0
1	10.0	55.2	98.9
2	2.14	22.8	33.0

TABLE 4 - TRIPPING STRESS COEFFICIENTS FOR TEES UNDER END LOADS AND MOMENTS WITH ROTATIONAL RESTRAINT

Tee Stiffener			
Mode m	R_c	Tripping Stress Coefficient $[(\sigma_e)_{cre} \times 10^4]/E$	
		Finite Element	Eqn. (21)
1	0	26.4	26.3
2	0	65.9	72.6
1	0.826	45.3	48.0
2	0.0748	73.3	78.0
1	1.65	56.4	69.7
2	0.150	77.7	83.4
1	4.96	75.5	156.6
2	0.449	85.6	105.2
1	8.26	82.7	243.5
2	0.748	88.6	126.9
Mode m	R_c	Tripping Moment Coefficient $\left[M_{cre}\left(d_c - h + \frac{1}{2}t\right) \times 10^4\right] \Big/ [IE]$	
		Finite Element	Eqn. (35)
1	0	29.4	29.0
2	0	75.1	80.1
1	0.826	49.7	53.0
2	0.0748	82.1	86.0
1	1.65	61.4	76.9
2	0.150	86.3	92.0

TABLE 5 - TRIPPING LOAD COEFFICIENTS UNDER UNIFORM LATERAL LOAD WITH ROTATIONAL RESTRAINT

Flat Bar

Mode m	R_c	B.C.*	Tripping Load Coefficient $100\, q_{cre} \dfrac{a^2\left(d-h+\frac{1}{2}t\right)}{EI}$	
			Finite Element	Eqn. (47)
1	0	SS	- 1.13	- 1.12
2	0	SS	- 1.20	- 1.18
1	0	C	+ 1.76	+ 1.96
2	0	C	+ 3.18	+ 3.90
2	0.427	SS	- 1.49	- 1.53
3?	0.153	SS	- 1.53	- 1.61
1	2.0	C	+ 3.15	+ 4.34
2	0.427	C	+ 3.69	+ 4.91
3?	0.764	SS	- 1.89	- 2.21
4?	0.338	SS	- 1.91	- 2.30
2	2.14	C	+ 4.49	+ 8.35
3?	0.764	C	+ 4.36	+ 8.18

Tee Stiffener

Mode m	R_c	B.C.*	Tripping Load Coefficient $100\, q_{cre} \dfrac{a^2\left(d_c-h+\frac{1}{2}t\right)}{EI}$	
			Finite Element	Eqn. (46)
1	0	SS	- 4.59	- 5.20
2	0	SS	- 9.03	-10.09
1	0	C	+ 6.54	+ 7.91
2	0	C	+17.91	+40.76
1	0.826	SS	- 6.70	- 8.75
2	0.0748	SS	- 9.65	-10.79
1	0.826	C	+10.7	+13.3
2	0.0748	C	+20.1	+42.7
1	8.26	SS	-10.1	-20.7
2	0.748	SS	-11.0	-16.8
1	8.26	C	+17.3	+46.2
2	0.748	C	+24.4	+58.3

*B.C. = Boundary Conditions, SS = Simple Support, C = Clamped.

? - Indicates uncertainty as to mode number.

significant source of error for the case of lateral loading, particularly positive pressure, is the distribution of out-of-plane displacements in the x-direction as defined by Equation (40). The presence of this source of error is most detectable in these examples for flat bars having zero rotational restraint about their line of attachment since, in this situation, little if any distortion of the web occurs and, therefore, the lack of close agreement with the finite element results cannot be ascribed to the neglect of web deformation.

Despite these discrepancies noted, Equation (40) does a good job, qualitatively at least, in describing the tripping phenomena for modes m = 1 and m = 2 when rotational restraint is nonexistent or very small. As rotational restraint increases, the tripping patterns become increasingly complex and soon this complexity reaches a stage where it is exceedingly difficult to associate a specific mode number with a particular buckling pattern, as the question marks appearing in Table 5 indicate. This is due to the concentration of tripping deformations in the regions of the stiffener undergoing compressive loading, with strongly attenuated or no deformations at all in those regions experiencing tension. Thus, tripping deformations under negative lateral loading will tend to be concentrated in the midsection of the stiffener while those associated with positive lateral loading will be concentrated at the two ends. In fact, for positive lateral loading and practical geometries (assuming there is sufficient vertical fixity to produce regions of compressive stresses) there are effectively only two buckling modes, one symmetrical and the other antisymmetrical about the stiffener midpoint. As the degree of rotational restraint increases, the deformations associated with both modes become more and more concentrated towards the ends until for large degrees of restraint (particularly for long stiffeners) the buckling patterns may be completely localized in the compression regions. As the buckling patterns become more localized, the corresponding tripping loads approach a common value. Consequently, for long stiffeners (large a/d) with moderate to high rotational restraint, the tripping load for both modes are effectively identical with the mode shapes essentially differing only with regard to their conditions of symmetry.

The rapidly deteriorating accuracy of the tripping solutions described in this section as rotational restraint increases, clearly indicates, even though based on very limited geometries and data, that these solutions are at best suitable for problems with zero or very limited amounts of such restraint. Because of the number of variables involved, parametric studies would be required to effectively define the degree of rotational restraint below which an acceptable level of accuracy could be guaranteed. Since the use of finite element programs in such studies can present significant economic stumbling blocks, an alternate approach was adopted which led to the development of approximate analytical solutions which take into account web deformations and are suitable for either hand calculation or programming on desk-top computers. These solutions are described and evaluated in the next section. Unfortunately these solutions are available only for the cases of axial end load and constant moment, and not for lateral loading. Consequently, semiempirical solutions will probably have to be developed for tripping under lateral load, making use of the analytical work presented here, finite element results, and any other relevant data available, at least until an improved analytical solution for this particular loading case is developed.

EFFECTS OF WEB DEFORMATIONS

In the previous development the critical assumption was made that the centerline of the web at any transverse cross section would not curve, i.e., for small deflections, $v \approx z\beta$. As the selected finite element solutions have demonstrated, however, this assumption in certain circumstances can lead to buckling predictions which are considerably higher than the true values. Since the proportions of the two stiffener examples studied are not untypical of ship-type structures, it is clear that solutions which take into account web deformations would be most valuable.

If the web is allowed to curve, then for small deformations the displacement of any point on the centerline of the web can be described in terms of a translation v and a rotation β. If a deformation function is assumed for the web, then the displacement of any point on the web centerline can be described in terms of the v and β of a single chosen point, in this case the shear center, as shown in Figure 7. (In the following development the location of the shear center is assumed to be at the intersection of the web and flange centerlines, i.e., $\bar{s} \approx d_c$, and although only approximately true, the shear center is indeed very close to this point for stiffeners with flanges of typical proportions and the consequences of this approximation are insignificant.) A logical deformation function is that of a beam, cantilevered at one end (the flange end)

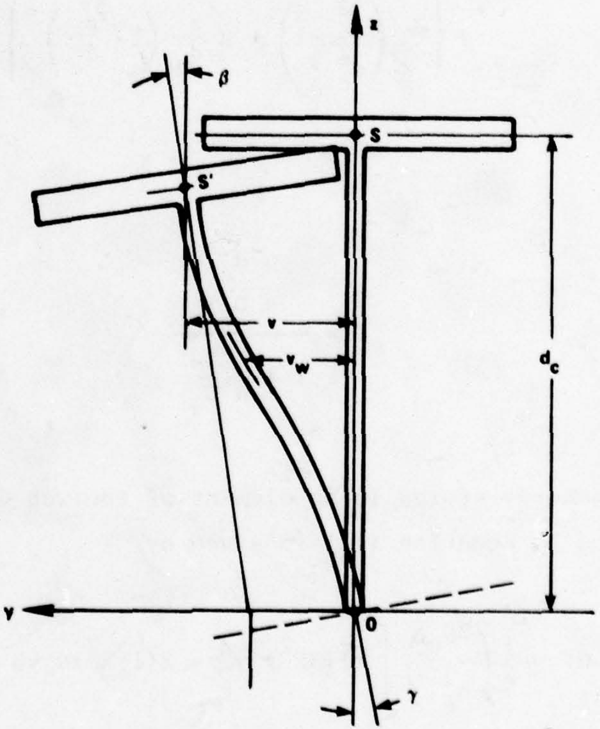

$$v_w = \frac{1}{2}\left[\left\{\frac{z}{d_c}\left(3 - \frac{z^2}{d_c^2}\right) - 3R\,\frac{z}{d_c}\left(1 - \frac{z}{d_c}\right)^2\right\} v + \left\{\frac{z}{d_c}\left(\frac{z^2}{d_c^2} - 1\right) + R\,\frac{z}{d_c}\left(1 - \frac{z}{d_c}\right)^2\right\} d_c\beta\right]$$

Figure 7 - Characterization of Web Deformations

and loaded by a concentrated force and moment at the other (corresponding to the restraining force and moment generated by the plating to which the stiffener is attached). In terms of the v and β displacements of the shear center this assumption gives the following expression for the lateral displacement v_w of any point on the stiffener web,

$$v_w = \frac{1}{2}\left[\left\{\frac{z}{d_c}\left(3-\frac{z^2}{d_c^2}\right) - 3R\,\frac{z}{d_c}\left(1-\frac{z}{d_c}\right)^2\right\} v + \left\{\frac{z}{d_c}\left(\frac{z^2}{d_c^2}-1\right) + R\,\frac{z}{d_c}\left(1-\frac{z}{d_c}\right)^2\right\} d_c\beta\right] \tag{57}$$

where

$$R = \frac{\dfrac{C\,d_c}{4\,D_w}}{1+\dfrac{C\,d_c}{4\,D_w}} \tag{58}$$

The strain energy stored in an element of the web due to its deformation as described by Equation (57) is given by

$$dV = \frac{1}{2}\left(\frac{3D_w}{d_c^3}\right)\left[(1+3R^2)\,v^2 - 2(1+R^2)d_c v\beta + \left(1+\frac{1}{3}R^2\right)d_c^2\beta^2\right]dx \tag{59}$$

The total strain energy stored in the structure in its buckled state is thus

$$V = \frac{1}{2}\int_0^a \Bigg[EI_z v_{xx}^2 + E\Gamma\beta_{xx}^2 + GJ\beta_x^2 + C\gamma^2 + \frac{3D_w}{d_c^3}\left\{(1+3R^2)\, v^2 - 2(1+R^2) d_c v\beta + \left(1 + \frac{1}{3}R^2\right) d_c^2\beta^2 \right\} \Bigg] dx \tag{60}$$

where γ is the rotation of the stiffener base (and thus the elastic spring) as shown in Figure 7. It is not difficult to show that

$$\gamma = \frac{1}{2\left(1+\frac{Cd_c}{4D_w}\right)}\left(3\,\frac{v}{d_c} - \beta\right) \tag{61}$$

and, therefore, V completely in terms of v and β is given by

$$V = \frac{1}{2}\int_0^a \Bigg[EI_z v_{xx}^2 + E\Gamma\beta_{xx}^2 + GJ\beta_x^2 + \frac{D_w}{d_c^3} R(1-R)\,(9v^2 - 6d_c v\beta + d_c^2\beta^2) + \frac{3D_w}{d_c^3}\left\{(1+3R^2)\, v^2 - 2(1+R^2)\, d_c v\beta + \left(1+\frac{1}{3}R^2\right) d_c^2\beta^2\right\} \Bigg] dx \tag{62}$$

If the stiffener is loaded by an axial inplane force, the potential energy of the loading in this case is the negative of the work done by that loading, namely

$$U_w = -W = -\iint \sigma_x\, \delta(y,z)\,dydx \tag{63}$$

Substituting $v_w\big|_{z=d_c} = v$ and $w = -y\beta$ for the flange, $w = 0$, and the deformation function v_w for the web into Equation (15) for $\delta(y,z)$ leads to

$$U_w = -\frac{1}{2}\int_0^a \sigma_e \Bigg[\left\{A_s - d_c t_w\left(\frac{18}{35} + \frac{19}{140}R - \frac{3}{140}R^2\right)\right\} v_x^2 - 2\left\{d_c^2 t_w\left(\frac{3}{35} - \frac{17}{420}R + \frac{1}{140}R^2\right)\right\} v_x\beta_x + \left\{I_{ps} - d_c^3 t_w\left(\frac{11}{35} + \frac{1}{84}R - \frac{1}{420}R^2\right)\right\} \beta_x^2\Bigg] dx \tag{64}$$

where I_{ps} is the polar moment of inertia of the stiffener about its shear center. This quantity can be computed from I_p according to

$$I_{ps} = I_p + A_s d_c^2 - 2 A_s d_c \bar{z} \tag{65}$$

where $\bar{z}$ is the height of the stiffener's centroid above its toe.

The total potential energy is the sum of the expressions (62) and (64),

$$U = V + U_w \tag{66}$$

and it can symbolically be represented by an integral of the form

$$U = \int_0^a \Phi(x, v, \beta, v_x, \beta_x, v_{xx}, \beta_{xx}) dx \tag{67}$$

The theory of stationary potential energy requires the integral in Equation (67) to be a minimum. This leads to two Eulerian differential equations,

$$\Phi_v - \frac{d}{dx}\Phi_{v_x} + \frac{d^2}{dx^2}\Phi_{v_{xx}} = 0 \qquad (68a)$$

$$\Phi_\beta - \frac{d}{dx}\Phi_{\beta_x} + \frac{d^2}{dx^2}\Phi_{\beta_{xx}} = 0 \qquad (68b)$$

where the subscript indicates a partial derivative with respect to that parameter.

Carrying out the operations indicated by the above expressions and assuming solutions for v and β of the form

$$v = v_o \sin\frac{m\pi x}{a} \text{ and } \beta = \beta_o \sin\frac{m\pi x}{a} \qquad (69)$$

leads to a set of two homogeneous equations for the constants v_o and β_o. Nonvanishing solutions for v_o and β_o can only exist if the determinant of the coefficients of these equations is zero. Computing this determinant results in a quadratic equation for the critical buckling stress, $(\sigma_e)_{cre}$,

$$(\sigma_e)^2_{cre}\,(k_2k_4-k_6^2) + (\sigma_e)_{cre}\,(k_1k_4+k_2k_3-2k_5k_6) + (k_1k_3-k_5^2) = 0 \qquad (70)$$

where the k_j's are given by

$$k_1 = EI_z\left(\frac{m\pi}{a}\right)^2 + 3\,\frac{D_w}{d_c^3}\left(\frac{a}{m\pi}\right)^2 (1+3R) \qquad (71a)$$

$$k_2 = -A_s + d_c t_w\left(\frac{18}{35} + \frac{19}{140}R - \frac{3}{140}R^2\right) \qquad (71b)$$

$$k_3 = GJ + E\Gamma\left(\frac{m\pi}{a}\right)^2 + \frac{3D_w}{d_c}\left(\frac{a}{m\pi}\right)^2\left(1+\frac{1}{3}R\right) \qquad (71c)$$

$$k_4 = - I_{ps} + d_c^3 t_w \left(\frac{11}{35} + \frac{1}{84} R - \frac{1}{420} R^2\right) \tag{71d}$$

$$k_5 = - \frac{3D_w}{d_c^2} \left(\frac{a}{m\pi}\right)^2 (1+R) \tag{71e}$$

$$k_6 = d_c^2 t_w \left(\frac{3}{35} - \frac{17}{420} R + \frac{1}{140} R^2\right) \tag{71f}$$

Using a similar procedure the critical load for tripping under constant moment can also be determined. This leads to a quadratic equation similar to Equation (70) for the critical moment M_{cre}, namely

$$M_{cre}^2 (\bar{k}_2\bar{k}_4 - \bar{k}_6^2) + M_{cre} (\bar{k}_1\bar{k}_4 + \bar{k}_2\bar{k}_3 - 2\bar{k}_5\bar{k}_6) + (\bar{k}_1\bar{k}_3 - \bar{k}_5^2) = 0 \tag{72}$$

The $\bar{k}_j$'s are closely related to the k_j's defined above, as indicated below,

$$\bar{k}_1 = \left(\frac{I}{d_c - h + \frac{1}{2} t}\right) k_1 \tag{73a}$$

$$\bar{k}_2 = k_2 + \frac{d_c^2 t_w}{d_c - h + \frac{1}{2} t} \left(\frac{159}{1120} - \frac{39}{560} R + \frac{3}{224} R^2\right) \tag{73b}$$

$$\bar{k}_3 = \left(\frac{I}{d_c - h + \frac{1}{2} t}\right) k_3 \tag{73c}$$

$$\bar{k}_4 = k_4 + \frac{d_c^4 t_w}{d_c - h + \frac{1}{2} t} \left(\frac{29}{3360} - \frac{11}{1680} R + \frac{1}{672} R^2\right) \tag{73d}$$

$$\bar{k}_5 = \left(\frac{I}{d_c - h + \frac{1}{2}\,t}\right) k_5 \qquad (73e)$$

$$\bar{k}_6 = k_6 - \frac{d_c^3 t_w}{d_c - h + \frac{1}{2}\,t}\left(\frac{113}{3360} - \frac{3}{140}\,R + \frac{1}{224}\,R^2\right) \qquad (73f)$$

Although the logic is clearly less soundly based, the web deformation function described by Equation (57) can also be applied to the problem of the tripping of flat bars. In this case, v and β represent not the displacement of the shear center, but rather that of the outer extremity of the flat bar. The strain energy is given by

$$V = \frac{1}{2}\,D_w \int_0^a \int_0^d \{[(v_w)_{xx} + (v_w)_{zz}]^2 - 2(1-\nu)[(v_w)_{xx}(v_w)_{zz} - (v_w)_{xz}^2]\}\,dxdz$$

$$+ \frac{1}{2}\int_0^a \frac{D_w}{d^3}\,R(1-R)\;(9v^2 - 6dv\beta + d^2\beta^2)\,dx \qquad (74)$$

while the potential energy U_w is identical to Equation (64) with the parameter d_c replaced by the flat bar depth d and I_{ps} replaced by the polar moment of inertia of the flat bar about its outer extremity $\left(= \frac{1}{3}\,d^3 t_w\right)$. The procedure followed to determine the critical stress is the same as that described previously and results in a quadratic equation identical to Equation (70). However, in this case, the k_j's are defined as follows:

$$k_1 = \frac{D_w}{d}\left(\frac{a}{md}\right)^2\left[\frac{3}{\pi^2}\,(1+3R) + \frac{3}{5}\left(\frac{md}{a}\right)^2 (4 - R + R^2)\right.$$

$$\left. + \pi^2\left(\frac{md}{a}\right)^4\left(\frac{17}{35} - \frac{19}{140}\,R + \frac{3}{140}\,R^2\right)\right] \qquad (75a)$$

$$k_2 = -\,dt_w\left[\frac{17}{35} - \frac{19}{140}\,R + \frac{3}{140}\,R^2 + \frac{1}{40}\,(4-R+R^2)\,(t_w/d)^2\right] \tag{75b}$$

$$k_3 = D_w d\left(\frac{a}{md}\right)^2\left[\frac{1}{\pi^2}\,(3+R) + \frac{1}{15}\left(\frac{md}{a}\right)^2(6-3R+R^2)\right.$$

$$\left. + \,\pi^2\left(\frac{md}{a}\right)^4\left(\frac{2}{105} - \frac{1}{84}\,R + \frac{1}{420}\,R^2\right)\right] \tag{75c}$$

$$k_4 = -\,d^3t_w\left[\frac{2}{105} - \frac{1}{84}\,R + \frac{1}{420}\,R^2 + \frac{1}{360}\,(6-3R+R^2)\,(t_w/d)^2\right] \tag{75d}$$

$$k_5 = -\,D_w\left(\frac{a}{md}\right)^2\left[\frac{3}{\pi^2}\,(1+R) + \left(\frac{md}{a}\right)^2\left(\frac{2}{5} + \nu - \frac{2}{5}\,R\right.\right.$$

$$\left.\left. + \,\frac{1}{5}\,R^2\right) + \pi^2\left(\frac{md}{a}\right)^4\left(\frac{3}{35} - \frac{17}{420}\,R + \frac{1}{140}\,R^2\right)\right] \tag{75e}$$

$$k_6 = +\,d^2t_w\left[\frac{3}{35} - \frac{17}{420}\,R + \frac{1}{140}\,R^2 + \frac{1}{120}\,(2-2R+R^2)\,(t_w/d)^2\right] \tag{75f}$$

For a constant moment, Equation (72) is applicable. In this case, however, the $\overline{k}_j$ functions are related to the k_j's defined as Equations (75a-75f) as follows:

$$\overline{k}_1 = \left(\frac{I}{d-h+\frac{1}{2}\,t}\right)k_1 \tag{76a}$$

$$\overline{k}_2 = k_2 + \frac{d^2t_w}{d-h+\frac{1}{2}\,t}\left[\frac{159}{1120} - \frac{39}{560}\,R + \frac{3}{224}\,R^2\right.$$

$$\left. + \,\frac{1}{48}\left(\frac{33}{10} - \frac{9}{5}\,R + \frac{9}{10}\,R^2\right)(t_w/d)^2\right] \tag{76b}$$

$$\bar{k}_3 = \left(\frac{I}{d-h+ \frac{1}{2}\ t} \right) k_3 \tag{76c}$$

$$\bar{k}_4 = k_4 + \frac{d^4 t_w}{d - h + \frac{1}{2}\ t} \left[\frac{29}{3360} - \frac{11}{1680} R + \frac{1}{672} R^2 \right.$$

$$\left. + \frac{1}{48} \left(\frac{3}{10} - \frac{4}{15} R + \frac{1}{10} R^2 \right) (t_w/d)^2 \right] \tag{76d}$$

$$\bar{k}_5 = \left(\frac{I}{d-h+ \frac{1}{2}\ t} \right) k_5 \tag{76e}$$

$$\bar{k}_6 = k_6 - \frac{d^3 t_w}{d - h + \frac{1}{2}\ t} \left[\frac{113}{3360} - \frac{3}{140} R + \frac{1}{224} R^2 \right.$$

$$\left. + \frac{1}{48} \left(\frac{4}{5} - \frac{7}{10} R + \frac{3}{10} R^2 \right) (t_w/d)^2 \right] \tag{76f}$$

While these solutions for flat bars are approximate, they have the advantage of not requiring an iterative solution (if b_e and C are known). An "exact" solution for end loading exists based on thin plate theory. The critical stress is determined from the solution of the equation

$$[c_1 \cos \beta d + c_2 \cosh \alpha d + c_3 c_2 \sinh \alpha d]\ [c_2\ \beta \cos \beta d$$

$$+ c_1\ \beta \cosh \alpha d] - [-c_2\ \beta \sin \beta d + c_1\ \alpha \sinh \alpha d$$

$$+ c_1 c_3\ \alpha \cosh \alpha d] \left[c_1 \sin \beta d + c_2 \frac{\beta}{\alpha} \sinh \alpha d \right] = 0 \tag{77a}$$

where, in this case

$$\left.\begin{aligned}
\alpha^2 &= \left(\frac{m\pi}{a}\right)^2 + \sqrt{\frac{\sigma_e t_w}{D_w}\left(\frac{m\pi}{a}\right)^2} \\
\beta^2 &= -\left(\frac{m\pi}{a}\right)^2 + \sqrt{\frac{\sigma_e t_w}{D_w}\left(\frac{m\pi}{a}\right)^2} \\
c_1 &= \beta^2 + \nu\left(\frac{m\pi}{a}\right)^2 \\
c_2 &= \alpha^2 - \nu\left(\frac{m\pi}{a}\right)^2 \\
&\text{and} \\
c_3 &= \left(\frac{\alpha^2+\beta^2}{\alpha C}\right) D_w
\end{aligned}\right\} \qquad (77b)$$

The obvious problem with this approach is that an iterative solution of a transcendental function is required, thus effectively eliminating it as a practical tool for hand calculation. Solution by computer is quite straightforward, nevertheless the necessity of an iterative solution may still be a serious drawback particularly in computer oriented design synthesis programs. Several levels of iterations may be required in such programs, thus resulting in the need for a single critical stress to be evaluated literally hundreds, or even thousands of times. In contrast, the solutions represented by Equations (70) and (72) are not inherently iterative by nature, and although admittedly cumbersome, are suitable for hand calculation. Even when the assumption that certain parameters, usually b_e and/or C, are load dependent requires an iterative solution, the manual use of these expressions is possible.

While solutions which take into account the influence of web deformations are available for the cases of axial end load and constant moment, unfortunately such solutions do not presently exist for the case of lateral loading as previously indicated. The difficulty is primarily due to the variation of σ_x with x and the inadequacy of a single sine function to represent the buckled shape. The lack of a solution for this particular loading case is particularly bothersome since the limited data presented in the previous section suggests a significant influence on buckling strength by web deformations. This problem is presently being investigated.

Using the same configurations previously discussed (see Figure 6), a series of comparisons were made between the solutions which include web deformations and those which do not. The results of these comparisons are presented and discussed in this section.

Tables 6 through 9 present buckling coefficients for both tee and flat bar stiffeners of constant length with varying degrees of rotational restrain about their toes. These tables clearly reemphasize behavior that was noted in the previous section, namely the increasing significance of web deformations on buckling strength as rotational restraint increases. These tables also indicate excellent agreement between the finite element solutions (the numbers on the tables in parentheses) and the approximate solutions represented by Equations (70) and (72) for all the degrees of restraint considered. With regard to the tee stiffener configuration, however, it is quite noticeable that for small or zero rotational restraint, Equations (70) and (72) predict somewhat lower (by several percent) buckling coefficients than do the finite element solutions. It would appear that this may be primarily due to the fact that in the finite element model the flange of the tee is modeled by a bar, which is a one-dimensional line element. Consequently, on computing the work W of the external forces, the finite element method is unable to include the effects on the parameters I_p and S (see Equations (20) and (34)) of the finite width and thickness of the flange. As the degree of rotational restraint increases, the data strongly suggest that the influence of this approximation decreases in significance.

TABLE 6 - TRIPPING STRESS COEFFICIENTS FOR TEES UNDER END LOADS WITH ROTATIONAL RESTRAINT

Tee Stiffener			
Mode m	R_c	Tripping Stress Coefficient $[(\sigma_e)_{cre} \times 10^4]/E$	
		Eqn. (70)*	Eqn. (21)
1	0	24.3 (26.4)	26.3
2	0	65.5 (65.9)	72.6
1	0.826	43.5 (45.3)	48.0
2	0.075	73.1 (73.3)	78.0
1	1.65	54.5 (56.4)	69.7
2	0.150	77.6 (77.7)	83.4
1	4.96	73.4 (75.5)	156.6
2	0.449	85.4 (85.6)	105.2
1	8.26	80.4 (82.7)	243.5
2	0.748	88.3 (88.6)	126.9
1	15.0	86.3	420.7
2	1.36	90.9	171.2

*Figures in parentheses are finite element values.

TABLE 7 - TRIPPING LOAD COEFFICIENTS FOR TEES UNDER END MOMENTS WITH ROTATIONAL RESTRAINT

Tee Stiffener			
Mode m	R_c	Tripping Moment Coefficient $\left[M_{cre}\left(d_c - h + \frac{1}{2}t\right) \times 10^4\right] / [IE]$	
		Eqn. (72)*	Eqn. (35)
1	0	27.1 (29.4)	29.0
2	0	74.6 (75.1)	80.1
1	0.826	47.7 (49.7)	53.0
2	0.075	81.7 (82.1)	86.0
1	1.65	59.3 (61.4)	76.9
2	0.150	85.9 (86.3)	92.0
1	4.96	78.9	172.8
2	0.449	93.1	116.0
1	8.26	86.0	268.6
2	0.748	95.8	139.9
1	15.0	92.0	464.0
2	1.36	98.2	188.8

*Figures in parentheses are finite element values.

TABLE 8 - TRIPPING STRESS COEFFICIENTS FOR FLAT BARS UNDER END LOADS WITH ROTATIONAL RESTRAINT

Flat Bar			
Mode m	R_c	Tripping Stress $[(\sigma_e)_{cre} \times 10^4]/E$ Coefficient	
		Eqn. (70)*	Eqn. (22)
1	0	6.42 (6.44)	6.42
2	0	7.51 (7.58)	7.51
1	1.00	12.44	12.84
2	0.214	9.10	9.12
1	2.00	17.6 (17.6)	19.3
2	0.427	10.5 (10.5)	10.7
1	5.00	29.3	38.5
2	1.07	13.6	15.5
1	10.0	41.5 (41.2)	70.6
2	2.14	17.0 (16.9)	23.6
1	15.0	49.1	102.7
2	3.20	19.1	31.6

*Figures in parentheses are finite element values.

TABLE 9 - TRIPPING LOAD COEFFICIENTS FOR FLAT BARS UNDER END MOMENTS WITH ROTATIONAL RESTRAINT

Flat Bar			
Mode m	R_c	Tripping Moment Coefficient $\left[M_{cre}\left(d-h+\frac{1}{2}t\right)\times 10^4\right] / [IE]$	
		Eqn. (72)*	Eqn. (36)
1	0	8.99 (9.04)	8.99
2	0	10.50 (10.66)	10.52
1	1.00	17.2	18.0
2	0.214	12.6	12.8
1	2.00	24.2 (24.3)	27.0
2	0.427	14.4 (14.6)	15.0
1	5.00	39.6	54.0
2	1.07	18.5	21.8
1	10.0	55.3 (55.2)	98.9
2	2.14	22.7 (22.8)	33.0
1	15.0	64.8	143.9
2	3.20	25.3	44.2

*Figures in parentheses are finite element values.

It was noted in the previous section that not only degree of rotational restraint but also stiffener proportions can influence the amount of web deformation which will be present. An example of this is illustrated in Table 10 where tripping stresses have been calculated for the tee stiffener of Figure 5 for varying lengths. It may be noted that as the length-to-depth ratio decreases there is an increasingly large discrepancy between the values of the tripping stresses predicted by Equations (21) and (70), indicating an increasing role of web deformation. As has been noted,[6] tripping for very short lengths is characterized by deformations consisting mainly of buckling of the web and twisting of the flange about its centerline. This is clearly a local buckling phenomena and its presence is indicated in Table 10 by these cases for which large discrepancies exist between the finite element results and those of Equation (70). These discrepancies occur because Equation (57), while an excellent approximation to the deformations which occur in the web during tripping, is a somewhat less than ideal approximation for local buckling of the web. Thus, while Equation (70) has been demonstrated to be reliable for predicting the primary tripping of tee stiffeners, it seems clear from this example that the possibility of local web buckling must be investigated by other means, such as plate theory.

For tee stiffeners, other geometrical parameters besides a/d_c can influence the amount of web deformation present. In a qualitative sense, the most significant factor involved seems to be the relative stiffnesses of flange versus web, since a stiff flange will tend to resist deformation, therefore, forcing more into the web. Many details of geometry can influence this ratio and thus, no further attempts will be made to examine them here. However, Table 11 illustrates the influence of length on degree of web deformation when there is no flange. The absence of any significant influence of length on tripping in this case in essence supports the hypotheses of the importance of flange versus web stiffness relative to web deformation.

TABLE 10 - TRIPPING STRESS COEFFICIENTS FOR TEES UNDER END LOADS WITH VARYING LENGTH/DEPTH RATIOS (NO ROTATIONAL RESTRAINT)

Tee Stiffener			
Mode m	$\frac{a}{md_c}$	Tripping Stress Coefficient $[(\sigma_e)_{cre} \times 10^4]/E$	
		Eqn. (70)*	Eqn. (21)
--	1.99	320.4 (193.1)	449.8
	2.66	217.4 (188.2)	257.7
--	3.99	107.8 (105.2)	120.6
	4.06	104.7 (102.5)	117.0
--	5.32	65.5 (65.8)	72.6
	7.48	38.3	42.1
--	8.11	34.2 (35.8)	37.4
	10.64	24.3 (26.4)	26.3
--	14.96	17.6	18.7
	16.62	16.3	17.2
--	33.24	12.2	12.4
*Figures in parentheses are finite element values.			

TABLE 11 - TRIPPING STRESS COEFFICIENTS FOR FLAT BARS UNDER END LOADS WITH VARYING LENGTH/DEPTH RATIOS (NO ROTATIONAL RESTRAINT)

Flat Bar			
Mode m	$\frac{a}{md}$	Tripping Stress Coefficient $[(\sigma_e)_{cre} \times 10^4]/E$	
		Eqn. (70)*	Eqn. (22)
--	1	20.3 (20.0)	20.3
	2	9.61 (9.51)	9.61
--	3.12	7.51 (7.47)	7.51
	4	6.95 (6.92)	6.95
--	5	6.62 (6.61)	6.62
	6.25	6.42 (6.41)	6.42
--	7.5	6.31 (6.30)	6.31
	10.0	6.20 (6.20)	6.20
--	15.0	6.12 (6.12)	6.12
	30.0	6.07 (6.07)	6.07
--			

*Values in parentheses from Equation (77).

TRIPPING UNDER COMBINED LOADING

The treatment of tripping to this point has considered both inplane and lateral loadings, but only applied individually. In many practical situations such loads will occur simultaneously which naturally leads to the subject of tripping under combined loading.

One approach to this problem is to follow the same procedure used for the individual loading cases, that is, to equate the strain energy associated with the assumed deformation function to the work done by the external loads. In this case, however, the work will include contributions from all the simultaneously occurring loads. One stress (or load) is then solved for (usually the predominant one) and thus becomes the tripping stress (or load) "in the presence of" the other applied loads.

As an example, consider the case of a tee stiffener loaded by both an axial end load and a uniform lateral load. Since a lateral load is present, the displacement function represented by Equation (40) must be used. The strain energy associated with this displacement function has previously been computed, but is repeated here,

$$V = \frac{1}{4}\, a\, \beta_o^2 \left(\frac{\pi}{a}\right)^2 GJ\, H_m(K) \tag{78}$$

for convenience. The work done by the lateral load has also been previously determined,

$$W_q = -\frac{1}{48}\left(\frac{q}{I}\right) \beta_o^2\, \pi^2\, a\, S\, F_m(K) \tag{79}$$

but here it is represented by the symbol W_q to indicate it is the component due to the lateral load. Equation (20) gives the work done by the axial end load for the assumed displacement function given by Equation (12); for displacement Equation (40) the appropriate work expression becomes

$$W_P = \frac{1}{4}\, \sigma_e\, \beta_o^2 \left(\frac{\pi}{a}\right)^2 a\, I_p [m^2K^2+(m+2)^2\ (K-1)^2] \tag{80}$$

The total work is the sum of the two components,

$$W = W_p + W_q$$

$$= \frac{1}{4}\,\sigma_e\,\beta_o^2\left(\frac{\pi}{a}\right)^2 a\, I_p\left[m^2K^2+(m+2)^2\,(K-1)^2\right]$$

$$- \frac{1}{48}\left(\frac{q}{I}\right)\beta_o^2\,\pi^2\, a\, S\, F_m(K) \qquad (81)$$

Equating the total work and the strain energy defines the condition of loading at which tripping will occur. If the axial end load is assumed to predominate, then carrying out the above procedure and solving for σ_e produces the following:

$$(\sigma_e)_{cre} = \frac{GJ\,H_m(K) + \frac{1}{12}\left(\frac{qa^2}{I}\right) S\,F_m(K)}{I_p\left[m^2K^2+(m+2)^2\,(K-1)^2\right]} \qquad (82)$$

As in the case of lateral load alone, the parameter K must be selected so that the resulting value of $(\sigma_e)_{cre}$ is the minimum. Since both the numerator and denominator of Equation (82) can be represented as quadratic functions of K, the procedure previously described for computing the appropriate value of K can also be applied here.

A second approach for computing tripping under combined loading involves the application of the so-called "interaction" formula. In this approach, for the type of loads considered here, tripping is assumed to occur when the following condition is satisfied:

$$\left[\frac{\sigma}{(\sigma_e)_{cre}}\right]^{\alpha} + \left[\frac{M}{M_{cre}}\right]^{\beta} + \left[\frac{q}{q_{cre}}\right]^{\gamma} = 1 \qquad (83)$$

In this expression $(\sigma_e)_{cre}$, M_{cre}, and q_{cre} are the failure "loads" corresponding to separate application of the three types of loads* considered (and all for the same mode number even though minimum failure loads for the different loads may occur for different modes). The indices α, β, and γ, while often suggested by theoretical considerations, are usually selected empirically on the basis of experimental and/or numerical results.

Limited calculations with expressions such as Equation (82), an example of which is illustrated in Figure 8 for the "tee" of Figure 6, suggest that for design purposes a linear interaction, as follows,

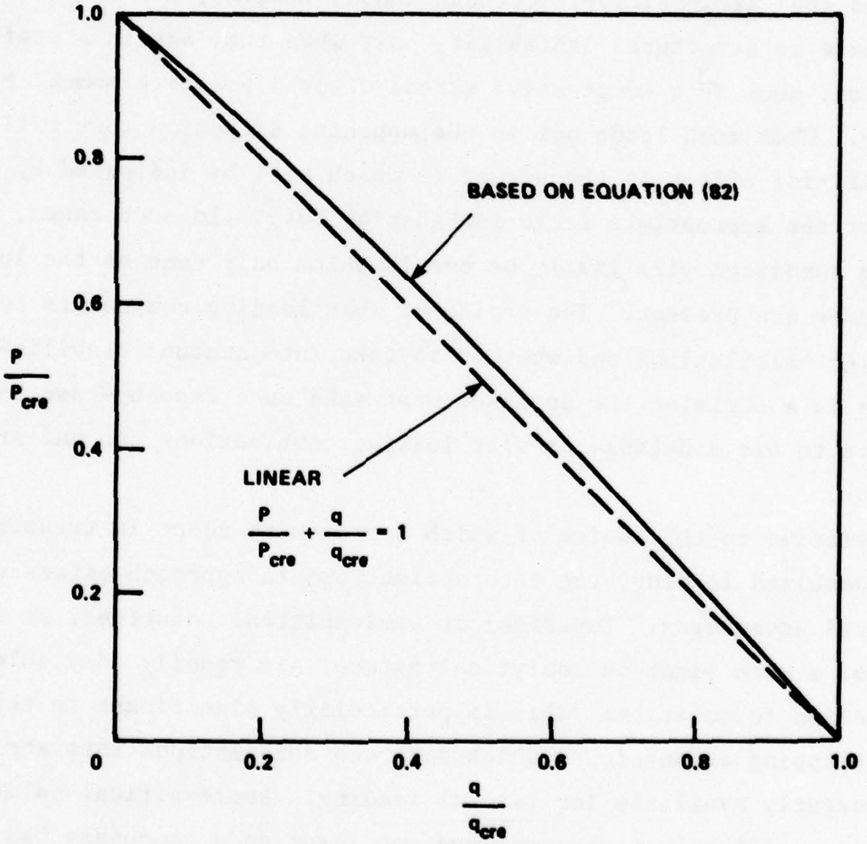

Figure 8 - Interaction Diagram for Combined Axial and Lateral Loads

---

*The distinction between M and the moments associated with q is the following. The moments associated with q arise due to local bending of the plate-beam between supporting transverses, whereas M is the moment component, approximately constant between adjacent transverses, due to overall grillage bending.

$$\frac{\sigma_e}{(\sigma_e)_{cre}} + \frac{M}{M_{cre}} + \frac{q}{q_{cre}} = 1 \qquad (84)$$

is the appropriate one to use. Although a bit conservative, this selection seems warranted until further evidence, either analytical or experimental, indicates a more realistic choice.

Generally speaking, the worst loading condition which can occur is one in which all the loads present are directed so as to have a destabilizing effect on the structure, i.e., the signs of all the ratios in Equation (84) are positive. Certain loads, however, may effectively contribute to structural instability only when they act in a preferred direction, such as a compressive stress σ_e or a positive moment M, for example. When such loads act in the opposite direction they will produce a stabilizing effect in the structure which will be indicated by a negative sign for the appropriate ratio in Equation (84). In such cases, the worst loading condition will likely be one in which only some of the loading components are present. The choice of what loading components to include in design calculations and whether to take into account stabilizing effects is a decision the designer must make on a case-by-case basis relative to his knowledge of what loading combinations can and are likely to occur.

Relative to the choice of which approach to adopt in treating tripping under combined loading, the interaction formula approach offers certain practical advantages. Empirical or semiempirical solutions, as well as those of a more vigorous analytical nature, are readily adaptable to an interaction formulation. This is particularly significant in this case since tripping expressions, which take web deformations into account, are not presently available for lateral loading. Semiempirical solutions, therefore, will have to be employed, at least on a temporary basis. The form of the interaction expression, through the indices α, β, and γ, also can readily accommodate the results of experimental investigations, if and when such data are available (and regardless of what values any analytical theories say such indices should assume). This great flexibility and the ease of application that the interaction formulation offers make this approach a very reasonable and practical choice for design applications.

ESTIMATION OF PLATE ROTATIONAL RESTRAINT

The numerous examples presented more than adequately illustrate the significant increases in tripping strength that rotational restraint along the toe of the stiffener provides. To take advantage of this added strength, it is necessary to be able to estimate the degree of rotational restraint that the plating, to which the stiffener is attached, provides.

One approach to this problem is to apply Rayleigh's principle as previously described but to include one frame spacing of plating in addition to the stiffener. When tripping occurs under axial end load the plating is assumed to deform laterally according to the expression

$$w = w_o \sin \frac{m\pi x}{a} \sin \frac{\pi y}{b} \qquad (85)$$

Since the junction of the stiffener web and the plating remain at right angles, this expression can readily be written in terms of the rotation β of the stiffener, giving

$$\begin{aligned} w &= \beta \left(\frac{b}{\pi}\right) \sin \frac{\pi y}{b} \\ &= \left(\beta_o \sin \frac{m\pi x}{a}\right) \left(\frac{b}{\pi}\right) \sin \frac{\pi y}{b} \qquad (86) \end{aligned}$$

Computing the strain energy of the plate-stiffener combination and the work done by the external forces and equating the two allows the critical tripping stress to be determined as follows,

$$(\sigma_e)_{cre} = \frac{GJ + E(I_z\bar{s}^2+\Gamma)\left(\frac{m\pi}{a}\right)^2 + \frac{tb^3}{2\pi^2}\,\sigma^m_{pbe}}{I_p + \frac{tb^3}{2\pi^2}\,\frac{\sigma^m_{pbe}}{(\sigma_e)^m_{pbe}}} \qquad (87)$$

where σ^m_{pbe} is the classical elastic plate buckling stress for mode number m,

$$\sigma^m_{pbe} = \frac{\pi^2 D}{tb^2}\left(\frac{a}{mb}\right)^2\left[1+\left(\frac{mb}{a}\right)^2\right]^2 \qquad (88)$$

and $(\sigma_e)^m_{pbe}$ is the peak value of stress (at the stiffener) at elastic plate buckling corresponding to a nonuniform distribution of stress in the y-direction. (When the distribution of stress in the y-direction is uniform, $(\sigma_e)^m_{pbe}$ *is equal to* σ^m_{pbe}.)

If it is assumed that the rotational spring constant of the plate interacts linearly with the axial inplane stress,

$$C = C_o\left[1-\frac{\sigma_e}{(\sigma_e)^m_{pbe}}\right] \qquad (89)$$

where C_o is the spring constant of the unloaded plate, then this relationship can be substituted into Equation (21) and a modified expression for $(\sigma_e)_{cre}$ determined. This gives

$$(\sigma_e)_{cre} = \frac{GJ + E(I_z\bar{s}^2+\Gamma)\left(\frac{m\pi}{a}\right)^2 + C_o\left(\frac{a}{m\pi}\right)^2}{I_p + \frac{C_o}{(\sigma_e)^m_{pbe}}\left(\frac{a}{m\pi}\right)^2} \qquad (90)$$

An examination of Equations (87) and (90) indicates that they are identical provided that

$$C_o \left(\frac{a}{m\pi}\right)^2 = \frac{tb^3}{2\pi^2} \sigma^m_{pbe} \qquad (91)$$

Solving the above expression for C_o and making use of Equation (88) provides the following

$$C_o = \frac{1}{2} \frac{\pi^2 D}{b} \left[1 + \left(\frac{mb}{a}\right)^2\right]^2 \qquad (92)$$

which, in combination with Equation (89), is the relationship being sought.

For practical applications, certain modifications of the above expressions are desirable at least until numerical and/or experimental validation of the theory can be provided. One such modification involves the use of the buckling stress $(\sigma_e)^m_{pbe}$ in Equation (89). This stress will not, in general, correspond to the minimum plate buckling stress since the mode number m used in determining $(\sigma_e)^m_{pbe}$ is the tripping mode number. This mode number will generally be lower than that corresponding to the minimum plate buckling stress, here denoted by $(\sigma_e)_{pbe}$. Although the problem is being investigated, there remains no clear understanding of the state of restraint (or destabilization) provided by the plating when the stress condition $(\sigma_e)_{pbe} < \sigma_e < (\sigma_e)^m_{pbe}$ holds. (Also, if the true tripping mode shape contains any Fourier components of the mode corresponding to the minimum stress plate buckling mode, it appears that linear theory would predict that the plate restraint would drop suddenly to zero as the minimum plate buckling stress is approached, although probably not in a linear manner.) Consequently, it is suggested that Equation (89) be modified to the following:

$$C = \begin{cases} C_o \left[1 - \dfrac{\sigma_e}{(\sigma_e)_{pbe}}\right] & \sigma_e < (\sigma_e)_{pbe} \\ 0 & \sigma_e \geq (\sigma_e)_{pbe} \end{cases} \qquad (93)$$

Since a conservative estimate of effective width will lead to an optimistically high (unconservative) estimate of $(\sigma_e)_{pbe}$ one further modification is called for, at least until more realistic values of effective width are routinely applied. This involves the use of the classical elastic plate buckling stress σ_{pbe}, defined by

$$\sigma_{pbe} = \frac{4\pi^2 D}{tb^2} \qquad (94)$$

in place of the value $(\sigma_e)_{pbe}$. This leads to the formulation for C:

$$C = \begin{cases} C_o \left(1 - \dfrac{\sigma_e}{\sigma_{pbe}}\right) & \sigma_e < \sigma_{pbe} \\ 0 & \sigma_e \geq \sigma_{pbe} \end{cases} \qquad (95)$$

If the conservatism of Equation (95) is viewed to be excessive, then a less conservative option is possible through the use of the average plate stress σ_a (not to be confused with the mean stress for the cross section σ_m) in place of σ_e in the above. However, it is significant to note that if the common practice of assuming a uniform distribution of primary stress for stress levels below plate buckling is adopted, then $\sigma_e = \sigma_a = \sigma_m$, $(\sigma_e)_{pbe} = \sigma_{pbe}$, and Equations (93) and (95) are identical.

Because of insufficient knowledge concerning the plating's behavior, one additional modification must be considered with regard to estimating the appropriate value of C. The expression for C_o, Equation (92), was derived on the basis of axial end loading and assumes that the tripping mode shape was a constant amplitude sinusoid. For axial end load and constant moment this is appropriate, but for lateral loading the more complicated tripping mode shapes which have been noted and described make the application of Equation (92) for $m > 1$ open to question. Discretion is obviously called for in this situation. Since C_o is a monotonically increasing function of m, one approach which can be adopted without fear of overly optimistic predictions is to use the minimum value of C_o, corresponding to $m = 1$, namely

$$C_o = \frac{1}{2}\,\frac{\pi^2 D}{b}\left[1+\left(\frac{b}{a}\right)^2\right]^2 \tag{96}$$

for all mode numbers. While this "minimum restraint" approach will obviously result in conservative predictions in some instances, its application will still offer the potential for significant increases in tripping strength since the greatest relative increases are associated with the initial increments of rotational stiffness. Until additional research clarifies these issues, this approach is recommended.

INELASTIC EFFECTS

Structures, in general, will begin to exhibit nonlinear behavior at stress levels below the yield point due to the presence of stress concentrations, fabrication distortions, residual stresses, etc. As a result of the tremendous complexities involved in treating this problem in a rigorous manner, there is, at present, no completely satisfactory method for considering the inelastic tripping of stiffeners welded to continuous plating, particularly for application to structural design calculations. It is possible, however, to apply some simple "corrections" to the elastic solutions previously derived which are intended in a gross manner to approximate the effect of such nonlinear behavior on the tripping strength of plate-stiffener combinations.

The approach, which is described in more detail elsewhere,[3] involves the application of a parameter referred to as the structural proportional limit ratio p_r. This ratio is defined as

$$p_r = \sigma_{ps}/\sigma_Y \tag{97}$$

where σ_{ps} is the structural proportional limit stress and σ_Y is the material tensile yield stress. A value of $p_r \approx 0.5$ is typical for welded ships.[3]

Assuming that the inelastic tripping stress $(\sigma_e)_{cr}$ is given by

$$(\sigma_e)_{cr} = \frac{E_t}{E} (\sigma_e)_{cre} \tag{98}$$

and approximating the ratio E_t/E using the Ostenfeld-Bleich quadratic parabolae

$$\frac{E_t}{E} = \frac{\sigma(\sigma_Y - \sigma)}{\sigma_{ps}(\sigma_Y - \sigma_{ps})} \tag{99}$$

leads to the following tripping strength expressions:

$$(\sigma_e)_{cr} = \begin{cases} (\sigma_e)_{cre} & (\sigma_e)_{cre} \le p_r \sigma_Y \\ \sigma_Y \left[1 - p_r(1-p_r) \dfrac{\sigma_Y}{(\sigma_e)_{cre}} \right] & \\ & (\sigma_e)_{cre} > p_r \sigma_Y \end{cases} \tag{100}$$

Although the nonuniform stress distribution renders the situation considerably more complex, this general approach can also be applied to the case of constant moment or uniform lateral pressure. In one such treatment, Equation (100) is still used, although, in these cases, $(\sigma_e)_{cre}$ is replaced by the maximum compressive bending stress corresponding to either M_{cre} or q_{cre} obtained by dividing the bending moment by the section modulus Z of the plate stiffener section. The difficulty with this approach is that it inherently implies that some sort of major structural "failure" will occur when the maximum compressive stress in the outer fiber of the stiffener reaches the material yield stress. This is clearly a conservative assumption. An alternative approach might be to assume that the inelastic tripping moment M_{cr} is given by

$$M_{cr} \approx \frac{(EI)_t}{EI} M_{cre} \qquad (101)$$

where $(EI)_t$ might be called a "tangent stiffness." Approximating the ratio $(EI)_t/EI$ in a manner similar to that of Equation (99) for E_t/E will lead to the following expressions for inelastic tripping moment

$$M_{cr} = \begin{cases} M_{cre} & M_{cre} \leq p_r M_p \\ M_p \left[1 - p_r (1 - p_r) \dfrac{M_p}{M_{cre}} \right] & M_{cre} > p_r M_p \end{cases} \qquad (102)$$

In these expressions M_p is the fully plastic moment for the plate-stiffener combination and p_r, while still a structural proportional limit ratio, now represents the ratio of the "proportional limit moment" (the value of the moment beyond which the moment-curvature relationship of the plate-stiffener begins to behave in a nonlinear fashion) to the fully plastic moment. Although there is little specific data to indicate a value for p_r in this case, a value of $p_r \approx 0.5$ as recommended for use in Equation (100) would seem to be a reasonable choice with which to start.

The degree to which M_{cr} obtained from Equation (102) will differ from that obtained from Equation (100) is primarily dependent on the shape factor of the plate-stiffener combination. The shape factor is the ratio of the fully plastic moment of the cross section to the moment required to cause initial yielding. For stiffeners which have much of their cross sectional area concentrated in the flange, the shape factor will take on values not much greater than 1 and, consequently, the differences resulting from using the two approaches will be minimal. For flat bars, however, the shape factor will take on greater values and the corresponding differences between computed values of the inelastic tripping moment will be more substantial. For example, the shape factors for the cross sections illustrated in Figure 5 are 1.72 for the flat bar and 1.30 for the tee.

A similar approach can also be applied in the case of combined loading, with the inelastic "correction" being applied to the stresses corresponding to the predominant loading. Thus, where uniform compressive loading is predominant, Equation (84) would be solved for σ (which in this case would represent the critical elastic tripping stress in the presence of the other loadings) and this stress then substituted in Equation (100) in place of $(\sigma_e)_{cre}$.

Since tripping stresses must often be calculated using an iterative scheme (when plate rotational restraint is included) there are two possible approaches for including the inelastic correction. One approach involves carrying out the iterations "completely elastically," including the use of σ_{pbe} in Equation (95) for C, and then applying the inelastic modification to the converged solution. The alternate approach involves applying the inelastic modification within each iterative cycle. In this case it would appear reasonable to use σ_{pb}, the inelastic plate buckling stress, rather than σ_{pbe}, in Equation (95). By replacing $(\sigma_e)_{cre}$ with σ_{pbe}, Equation (100) can also be used to compute the necessary value of σ_{pb}.

CONCLUSIONS

This report describes the application of classical energy theory to the problem of developing design oriented techniques for predicting the lateral torsional (tripping) instability of plate-stiffener combinations. Closed form solutions have been developed which show excellent agreement with numerical results generated using the finite element method for axial end loading and constant moment, but which are less universally reliable in treating plate-stiffeners under uniform lateral loading.

The comparative solutions made with the finite element analyses have very clearly illustrated the importance of including the effects of web deformations, particularly for the stiffeners possessing substantial flanges. Solutions which ignore these effects have been shown to retain acceptable accuracy only when the rotational restraint present along the stiffeners line of attachment to the plating is nonexistent or very small. In the course of the development this discovery provided the inspiration which eventually resulted in the derivation of solutions for tripping under axial end load and constant moment, including the effects of web deformation. These solutions have provided tripping load predictions which are in excellent agreement with the corresponding finite element analyses for the complete range of rotational restraints considered. They are clearly more cumbersome to use in hand calculations than the more simplified (and less accurate) expressions, but their complexity does not preclude their effective use in manual calculations, particularly in view of the increasing capability and sophistication of hand-held calculators and desk top mini-computers. These solutions are obviously ideally suited for programming on digital computers and thus should be extremely effective when incorporated into large structural synthesis programs whose primary applications are in the preliminary stages of structural design.

The major problem area encountered in this study is that of estimating the critical values for tripping under lateral loading. For the solutions presented, errors which range approximately from 0 to 20 percent can reasonably be expected for the primary tripping mode ($m=1$) with zero or extremely limited rotational restraint. For larger degrees of rotational restraint and the higher modes which are a natural consequence, the corresponding errors are appreciably larger. The inability at present to take web deformations into account and to adequately model the generally more complex modal shapes (apart from the web deformation aspect) are the primary culprits. These difficulties, in turn, are related to the functional dependence of the σ_x stress on the x-coordinate. Until more satisfactory analytical solutions are developed, either semiempirical solutions based on the theory presented here and numerical analysis, or finite element programs directed specifically at the tripping problem, will have to be utilized.

Several other areas for which further study is required have been indicated, or at least alluded to, in the main text. With regard to the estimation of plate rotational restraint, several problem areas can be identified: (1) the estimation of restraint for the more complex tripping mode shapes which occur when lateral loading is present, (2) an improved definition of the influence of plate buckling on plating restraint, and (3) the effect of post buckling behavior of the plating on stiffener tripping. Inelastic tripping behavior is another very fertile area for further research. It is difficult to be specific in this area since the present design oriented techniques as outlined here are extremely crude and a careful examination of the whole area is easily justified. Tripping of nonuniform and unsymmetrical stiffeners are also subjects of major and practical interest. This "wish list" is not all-inclusive, nor is it intended to be, but it should clearly indicate that there are certainly many questions remaining to be answered with regard to the tripping phenomenon.

The ultimate goal of this study being design applications, this report would not be complete without consideration of the current Navy design practice relative to stiffener tripping. In this design practice[8] the maximum ratio of stiffener span to flange width (a/f_w), for which support is required only at the ends, is given by

$$\left(\frac{a}{f_w}\right) = \frac{\left(\frac{\pi}{\sqrt{6}}\right)\sqrt{\frac{E}{\sigma_Y}}}{\sqrt{1+\frac{1}{3}\left(\frac{d}{f_w}\right)\left(\frac{t_w}{t_f}\right)-\left(\frac{E}{7.8\ \sigma_Y}\right)\left(\frac{t_f}{f_w}\right)^2\left(\frac{f_w}{d}\right)^2}} \tag{103}$$

If the following approximations are made,

$$\begin{aligned} I_z &\approx \frac{1}{12}\, t_f f_w^3 \\ I_p &\approx t_f f_w d^2 + \frac{1}{3}\, t_w d^3 \\ \bar{s} &\approx d \\ J &\approx \frac{1}{3}\, f_w t_f^3 \\ \Gamma &\approx 0 \end{aligned} \tag{104}$$

then Equation (103) can easily be shown to be identical to Equation (21) with $C = 0$, $(\sigma_e)_{cre} = \sigma_Y$, $\nu = 0.3$, and $m = \sqrt{2}$. The use of this criteria is designed to insure that stiffeners are proportioned such that tripping will not occur at any stress less than yield. This criteria is somewhat conservative since it is based on a theory for purely axial compression (whereas most stiffeners experience loading which is a combination of bending and axial compression) and it ignores the rotational restraint of the plating ($C=0$). Factors which offset this inherent conservatism to a small degree involve the selection of $m = \sqrt{2}$ and the neglect of web deformations. The value of m chosen is intended to reflect the degree of rotational restraint in the plane of the web anticipated at the ends of the stiffener. The neglect of web deformations in this case is not significant since, when plating restraint is also neglected, the effect of web deformations is in general quite small. It should also be noted that the criterion represented by Equation (103) is applicable only to tee stiffeners and for a number of reasons cannot be appropriately applied to flat bar stiffeners.

As a final comment, it has become quite common in reports of this type to decry the lack of experimental data which are available for validation of the theories presented. This report is no different. The value of good experimental data cannot be overestimated because any predictive techniques, no matter how sound their theoretical base, are only of value insofar as they are capable of describing what occurs in the real world. The development of confidence in the application of new technology in the design process will continue to be a painfully slow process without the validation only correlation with experimental data can provide.

ACKNOWLEDGMENTS

The author wishes to express his sincere appreciation to Dr. M.O. Critchfield and Mr. F.M. Lev for their helpful discussions and careful evaluations of the contents of this report.

APPENDIX A

SAMPLE PROBLEMS

Although the application of many of the expressions in the main text is perfectly straightforward, the use of sample problems can often be very enlightening, particularly when the solution procedure requires a number of steps.

Consider the plate-tee stiffener combination whose geometry is defined in Figure 6. A number of geometrical parameters require evaluation in order for the tripping loads to be determined. These parameters are defined in Figure 2 and for this example have the following values:

$$I_z = 58.79 \text{ cm}^4$$

$$\bar{s} = 14.98 \text{ cm}$$

$$\Gamma = 40.57 \text{ cm}^6$$

$$J = 9.34 \text{ cm}^4$$

$$I_p = 3306 \text{ cm}^4$$

ZERO ROTATIONAL RESTRAINT

If no rotational restraint is assumed, i.e., $C = 0$, then a reasonable value for the tripping stress for mode $m = 1$ under axial end loading may be found using Equation (21). Assuming values of $E = 6.894 \times 10^6$ N/cm^2 and $\nu = 0.3$ (which result in a value $G = 2.652 \times 10^6$ N/cm^2), this expression gives

$$(\sigma_e)_{cre} = \frac{1}{3306} [(2.652 \times 10^6)\ (9.34)$$

$$+ (6.894 \times 10^6)((58.79)\ (14.98)^2 + 40.57)\ (\pi/160)^2]$$

$$= 18{,}130 \text{ N/cm}^2 \qquad \text{(A.1)}$$

The procedure for determining the tripping load under lateral loading is somewhat more involved. First the coefficients of the $H_m(K)$ and $F_m(K)$ functions must be determined. The most convenient form of these expressions is provided in Appendix B. Using these expressions the h_j coefficients can be readily calculated, giving for mode m = 1 and C = 0 the following,

$$\begin{aligned} h_0 &= 124.0 \\ h_1 &= -248.0 \\ h_2 &= 126.4 \end{aligned} \tag{A.2}$$

To calculate the coefficients f_j, a few additional geometrical parameters (not previously defined here or in Figure 6) are required, namely

$$\begin{aligned} d_w &= 14.33 \text{ cm} \\ d_c &= 15.04 \text{ cm} \\ A_f &= 11.218 \text{ cm}^2 \\ I_{zf} &= 58.34 \text{ cm}^4 \end{aligned} \tag{A.3}$$

The parameter S, also required, is defined by Equation (33). This parameter thus takes on the value,

$$S = 29{,}890 \text{ cm}^5 \tag{A.4}$$

The coefficients f_j are also functionally dependent on the degree of vertical fixity of the stiffener ends. Considering first the simply supported case leads to the values,

$$\begin{aligned} f_0 &= 8.619 \\ f_1 &= -14.958 \\ f_2 &= 6.958 \end{aligned} \tag{A.5}$$

The coefficients h_j and f_j are used to compute the three coefficients of the quadratic equation in K, Equation (49). Using the above values, this results in the expression

$$165.1K^2 - 453.3K + 282.7 = 0 \tag{A.6}$$

for which two roots can readily be computed, namely

$$\begin{aligned} K_1 &= 1.788 \\ K_2 &= 0.958 \end{aligned} \tag{A.7}$$

The critical tripping loads corresponding to these two roots can now be readily calculated using Equation (46). This expression requires the vertical moment of inertia of the plate-stiffener combination which, through the routine computation, is found to be

$$I = 2071 \text{ cm}^4 \tag{A.8}$$

The functions $H_1(K)$ and $F_1(K)$ must also be evaluated. Using the two roots for K and the coefficients h_j and f_j previously defined, the following values result,

$$\begin{array}{lcc} & K_1 & K_2 \\ H_1(K) = & 84.67 & 2.421 \\ F_1(K) = & 4.118 & 0.675 \end{array} \tag{A.9}$$

Substitution of the above values into Equation (46) finally leads to the desired result, namely

$$q_{cre} = \begin{cases} -\ 16{,}540\ \text{N/cm} \\ \qquad \text{for } K = K_1 \\ -\ 2{,}885\ \text{N/cm} \\ \qquad \text{for } K = K_2 \end{cases} \tag{A.10}$$

Of these two values, the one corresponding to the root K_2 is the one of practical interest. The critical value corresponding to K_1 might be termed a "high energy" tripping load and, although mathematically possible, it represents a tripping condition which could never occur in the real structure.

For the case where the ends of the stiffener are clamped, the procedure is the same as previously described except that in this case the coefficients f_j take on the following values,

$$\begin{aligned} f_0 &= -0.381 \\ f_1 &= 3.042 \\ f_2 &= -3.042 \end{aligned} \tag{A.11}$$

These values and the coefficients h_j previously defined lead to the quadratic equation,

$$369.9K^2 - 658.1K + 282.7 = 0 \tag{A.12}$$

and the roots

$$\begin{aligned} K_1 &= 1.054 \\ K_2 &= 0.725 \end{aligned} \tag{A.13}$$

These roots, in turn, lead to the critical tripping loads

$$q_{cre} = \begin{cases} +\ 4{,}397\ \text{N/cm} \\ \qquad\qquad \text{for } K = K_1 \\ -\ 38{,}040\ \text{N/cm} \\ \qquad\qquad \text{for } K = K_2 \end{cases} \tag{A.14}$$

The occurrence here of tripping loads of both signs (positive and negative) indicates that tripping can occur due to loads acting in either direction, unlike the simply supported case. Thus, both of the above tripping loads represent realistic tripping phenomena. Which of these loads in any given situation is the one of practical interest will depend on the direction of the lateral loading or loadings under consideration.

FINITE ROTATIONAL RESTRAINT

If any but a very small amount of rotational restraint along the stiffener's line of attachment to the plating is to be considered, then the solutions for tripping which include web deformations should be utilized. For axial end loading this solution is given by Equation (70), the coefficients for which are provided by Equations (71). These expressions involve the additional parameters

$$\begin{aligned} D_w &= 2.376 \times 10^5 \text{ N-cm} \\ \bar{z} &= 11.26 \text{ cm} \\ A_s &= 21.56 \text{ cm}^2 \\ I_{ps} &= 880 \text{ cm}^4 \end{aligned} \tag{A.15}$$

as well as the dimensionless rotational restraint parameter, R. Assuming a rotational spring constant of the supporting plating of C = 30,000 N-cm/rad leads to a value for R of

$$R = 0.322 \tag{A.16}$$

For this value of R the coefficient k_j has the following values (for m=1),

$$
\begin{aligned}
k_1 &= 1.225 \times 10^6 \text{ N} \\
k_2 &= -15.53 \text{ cm}^2 \\
k_3 &= 1.610 \times 10^8 \text{ N-cm}^2 \\
k_4 &= -99.2 \text{ cm}^4 \\
k_5 &= -10.81 \times 10^6 \text{ N-cm} \\
k_6 &= 11.99 \text{ cm}^3
\end{aligned}
\tag{A.17}
$$

which lead to the quadratic equation

$$1397 (\sigma_e)^2_{cre} - (2.363 \times 10^9)(\sigma_e)_{cre} + (0.803 \times 10^{14}) = 0 \tag{A.18}$$

and finally, the roots

$$(\sigma_e)_{cre} = \begin{cases} 1.66 \times 10^6 \text{ N/cm}^2 \\ 34{,}700 \text{ N/cm}^2 \end{cases} \tag{A.19}$$

The root of interest is the second one; the first root represents a solution mode which is mathematically but not physically possible.

For the case of lateral loading, solutions which include the effects of web deformations are not presently available. Consequently, to treat this case one has the choice of ignoring the influence of the rotational resistance, or if this course is not preferable, of making use of an available finite element program. Finite element results for the problem being examined here are presented in Table 5 in the main text for several values of rotational resistance.

INELASTIC EFFECTS

If the material has a yield stress of $\sigma_Y = 20{,}000$ N/cm^2 and a structural proportional limit ratio $p_r = 0.5$ is assumed, then the axial end loading solutions for both zero and finite rotational resistance should be adjusted for inelastic effects according to Equation (100). For $p_r = 0.5$, this expression becomes

$$(\sigma_e)_{cr} = \begin{cases} (\sigma_e)_{cre} & (\sigma_e)_{cre} \leq \frac{1}{2}\sigma_Y \\ \sigma_Y \left[1 - \frac{\sigma_Y}{4(\sigma_e)_{cre}}\right] & \\ & (\sigma_e)_{cre} > \frac{1}{2}\sigma_Y \end{cases} \tag{A.20}$$

Thus for zero rotational restraint, the inelastic tripping stress becomes

$$\begin{aligned}(\sigma_e)_{cr} &= 20{,}000 \left[1 - \frac{20{,}000}{4 \times 18{,}130}\right] \\ &= 14{,}480 \text{ N/cm}^2\end{aligned} \tag{A.21}$$

and for C = 30,000 N-cm/rad

$$\begin{aligned}(\sigma_e)_{cr} &= 20{,}000 \left[1 - \frac{20{,}000}{4 \times 34{,}700}\right] \\ &= 17{,}120 \text{ N/cm}^2\end{aligned} \tag{A.22}$$

If the "effective width" for plating effectiveness under inplane loading is also assumed, in this example, to be equal to 30.5 cm and the stiffener spacing b = 45 cm, then the mean inelastic tripping stresses can be computed according to Equation (27). This expression gives

$$\begin{aligned}(\sigma_m)_{cr} &= \frac{21.56 + (30.5 \times 0.8)}{21.56 + (45.0 \times 0.8)} \times 14{,}480 \\ &= 11{,}560 \text{ N/cm}^2\end{aligned} \tag{A.23}$$

for zero rotational restraint and

$$(\sigma_m)_{cr} = \frac{21.56 + (30.5 \times 0.8)}{21.56 + (45.0 \times 0.8)} \times 17{,}120$$

$$= 13{,}670 \text{ N/cm}^2 \tag{A.24}$$

for C = 30,000 N-cm/rad.

Since the classical plate buckling stress for the plating in this example (a=160 cm, b=45 cm, t=0.80 cm) according to Equation (94) is

$$\sigma_{pbe} = \sigma_{pb} = 7{,}880 \text{ N/cm}^2 \tag{A.25}$$

it should be immediately clear that iterations are unnecessary in this case and that the appropriate solution (assuming that the resistance represented by C is due to the plating) is the one corresponding to C = 0 (zero rotational restraint).

To examine how the iterative procedure is carried out, consider the same stiffener attached to plating 1.2 cm thick at a uniform spacing of 38 cm. In this case, the classical plate buckling stress (for a=160 cm, b=38 cm, t=1.2 cm) is

$$\sigma_{pbe} = 24{,}860 \text{ N/cm}^2 \tag{A.26}$$

Correcting this value for inelastic effects (using $p_r = 0.5$ here, also) gives

$$\sigma_{pb} = 15{,}980 \text{ N/cm}^2 \tag{A.27}$$

Since the dimensions of the plating do not enter into the calculations for $(\sigma_e)_{cre}$ and $(\sigma_e)_{cr}$, the previous values computed are also valid here.

Since C and $(\sigma_e)_{cr}$ are functionally related by Equation (95), the value of $(\sigma_e)_{cr}$ calculated for C = 30,000 N-cm/rad can be used as a "starting" value in the iteration process. The value of C_o used in Equation (95) is defined by Equation (96) which, in this case, has the value

$$C_o = 158{,}100 \text{ N-cm/rad} \tag{A.28}$$

Substituting the critical stress $(\sigma_e)_{cr} = 17{,}120$ N/cm^2 into Equation (95), produces

$$C = 158{,}100 \left(1- \frac{17{,}120}{15{,}980}\right) < 0$$

or (A.29)

$$C = 0$$

This value may now be used as the second estimate of C, or (hopefully) to minimize the number of cycles, a value may be selected which is somewhere in between the "assumed" (C=30,000) and "calculated" (C=0) values. Try C = 5,000 N-cm/rad for the second estimate. This gives

$$(\sigma_e)_{cre} = 21{,}070 \text{ N/cm}^2$$

(A.30)

$$(\sigma_e)_{cr} = 15{,}250 \text{ N/cm}^2$$

and, consequently,

$$C = 158{,}100 \left(1- \frac{15{,}250}{15{,}980}\right) = 7{,}220 \text{ N-cm/rad} \tag{A.31}$$

Now, assume C = 6,000 N-cm/rad. This results in

$$
\begin{aligned}
(\sigma_e)_{cre} &= 21{,}840 \text{ N/cm}^2 \\
(\sigma_e)_{cr} &= 15{,}420 \text{ N/cm}^2 \\
C &= 5{,}540 \text{ N-cm/rad}
\end{aligned}
\qquad (A.32)
$$

Now, assume C = 5,800 N-cm/rad. This results in

$$
\begin{aligned}
(\sigma_e)_{cre} &= 21{,}680 \text{ N/cm}^2 \\
(\sigma_e)_{cr} &= 15{,}390 \text{ N/cm}^2 \\
C &= 5{,}840 \text{ N-cm/rad}
\end{aligned}
\qquad (A.33)
$$

Because of the very slight changes in the tripping stresses $(\sigma_e)_{cr}$ between the last two cycles, practical considerations would dictate that the iteration process has converged sufficiently for engineering purposes. Thus, the final solutions, rounded off, are

$$
\begin{aligned}
(\sigma_e)_{cre} &= 21{,}700 \text{ N/cm}^2 \\
(\sigma_e)_{cr} &= 15{,}400 \text{ N/cm}^2
\end{aligned}
\qquad (A.34)
$$

COMBINED LOADING

Returning to the original problem (b=45 cm, b_e=30.5 cm, t=0.80 cm), consider the situation when both axial end loads and lateral loads are occurring simultaneously. In this case elastic tripping is assumed to occur when the expression

$$
\frac{\sigma_e}{(\sigma_e)_{cre}} + \frac{q}{q_{cre}} = 1 \qquad (A.35)
$$

is satisfied. If rotational restraint is ignored (C=0), then values of $(\sigma_e)_{cre}$ and q_{cre} (for clamped end conditions) have previously been computed. Thus, the above expression becomes

$$\frac{\sigma_e}{18,100} + \frac{q}{4,400} = 1 \qquad \text{(A.36)}$$

For a lateral loading of magnitude $q = 450$ N/cm (corresponding to a uniform pressure of 10 N/cm^2) the maximum bending stress in the flange of the stiffener will be on the order of 5,000 N/cm^2. Thus, at tripping, σ_e will be the predominant loading. Solving for σ_e and designating the result by $(\sigma_e)_{cre,q}$ to distinguish it from $(\sigma_e)_{cre}$, gives

$$\begin{aligned}(\sigma_e)_{cre,q} &= 18,100 \left(1- \frac{450}{4,400}\right) \\ &= 16,250 \text{ N/cm}^2\end{aligned} \qquad \text{(A.37)}$$

Since σ_e is the predominant loading, the inelastic correction is applied to $(\sigma_e)_{cre,q}$ resulting in

$$(\sigma_e)_{cr,q} = 13,850 \text{ N/cm}^2 \qquad \text{(A.38)}$$

The mean axial tripping stress is then

$$(\sigma_m)_{cr,q} = 11,060 \text{ N/cm}^2 \qquad \text{(A.39)}$$

APPENDIX B

QUADRATIC COEFFICIENTS FOR $H_m(K)$ AND $F_m(K)$ FUNCTIONS

The functions $H_m(K)$, $\overline{H}_m(K)$, and $F_m(K)$, defined in the main text in relation to laterally loaded beams, are quadratic functions of the scalar parameter K. Thus these functions can be written as

$$
\begin{aligned}
H_m(K) &= h_0 + h_1 K + h_2 K^2 \\
\overline{H}_m(K) &= \overline{h}_0 + \overline{h}_1 K + \overline{h}_2 K^2 \\
F_m(K) &= f_0 + f_1(K) + f_2 K^2
\end{aligned}
\qquad \text{(B.1)}
$$

The determination of the appropriate value of K requires that the specific coefficients h_i, $\overline{h}_i$, and f_i be identified. This can be readily accomplished simply by rearranging and collecting terms for each of the three functions. Therefore, from Equation (43a) one obtains

$$h_0 = (m+2)^2 + (m+2)^4 \frac{\pi^2 E}{a^2 GJ} (I_z s^{-2} + \Gamma) + \frac{a^2 C}{\pi^2 GJ} \qquad \text{(B.2a)}$$

$$h_1 = -\,2 \left[(m+2)^2 + (m+2)^4 \frac{\pi^2 E}{a^2 GJ} (I_z s^{-2} + \Gamma) + \frac{a^2 C}{\pi^2 GJ} \right] \qquad \text{(B.2b)}$$

$$h_2 = 2(m^2+2m+2) + [m^4 + (m+2)^4] \frac{\pi^2 E}{a^2 GJ} (I_z s^{-2} + \Gamma) + \frac{2a^2 C}{\pi^2 GJ} \qquad \text{(B.2c)}$$

Similarly, from Equation (43b), the coefficients for $\overline{H}_m(K)$ are defined

$$\overline{h}_0 = (m+2)^4 \left(\frac{\pi d}{a}\right)^2 + 6(m+2)^2 (1-\nu) + \frac{3a^2 C}{\pi^2 D_w d} \qquad \text{(B.3a)}$$

PRECEDING PAGE BLANK

$$\bar{h}_1 = -2\left[(m+2)^4\left(\frac{\pi d}{a}\right)^2 + 6(m+2)^2\ (1-\nu) + \frac{3a^2C}{\pi^2 D_w d}\right] \tag{B.3b}$$

$$\bar{h}_2 = [m^4+(m+2)^4]\left(\frac{\pi d}{a}\right)^2 + 12(m^2+2m+2)\ (1-\nu) + \frac{6a^2C}{\pi^2 D_w d} \tag{B.3c}$$

For the function $F_m(K)$, two sets of coefficients must be defined, one for the simply supported case and the other for the clamped case. For the simply supported case Equation (45) will yield

$$f_0 = (m+2)^2 - \frac{3}{\pi^2} - \frac{6d_w}{\pi^2 S}\left[A_f t_f\ \left(d_c - h + \frac{1}{2}\ t\right) + b_e t^2 h\right] \tag{B.4a}$$

$$f_1 = -\ 2(m+2)^2 + \frac{6}{\pi^2}\left[1+m(m+2)\ \left\{1+\frac{1}{(m+1)^2}\right\}\right]$$
$$+ \frac{12d_w}{\pi^2 S}\left[A_f t_f\ \left(d_c - h + \frac{1}{2}\ t\right)\ + b_e t^2 h\right] \tag{B.4b}$$

$$f_2 = m^2 + (m+2)^2 - \frac{6}{\pi^2}\left[1+m(m+2)\ \left\{1+\frac{1}{(m+1)^2}\right\}\right]$$
$$- \frac{12d_w}{\pi^2 S}\left[A_f t_f\ \left(d_c - h + \frac{1}{2}\ t\right) + b_e t^2 h\right] \tag{B.4c}$$

For the clamped case these coefficients become (from Equation (53))

$$f_0 = -\frac{3}{\pi^2} - \frac{6d_w}{\pi^2 S}\left[A_f t_f\ \left(d_c - h + \frac{1}{2}\ t\right) + b_e t^2 h\right] \tag{B.5a}$$

$$f_1 = \frac{6}{\pi^2}\left[1+m(m+2)\left\{1+\frac{1}{(m+1)^2}\right\}\right]$$

$$+\frac{12d_w}{\pi^2 S}\left[A_f t_f\left(d_c-h+\frac{1}{2}\,t\right)+b_e t^2 h\right] \qquad \text{(B.5b)}$$

$$f_2 = -\frac{6}{\pi^2}\left[1+m(m+2)\left\{1+\frac{1}{(m+1)^2}\right\}\right]$$

$$-\frac{12d_w}{\pi^2 S}\left[A_f t_f\left(d_c-h+\frac{1}{2}\,t\right)+b_e t^2 h\right] \qquad \text{(B.5c)}$$

(Note that in the expressions for the f_j, the symbol h for the location of the neutral axis should not be confused with the coefficients h_j previously defined.)

APPENDIX C

COMPARISONS WITH EXPERIMENTAL DATA

Although relevant experimental data on tripping failure are virtually nonexistant, the Naval Construction Research Establishment (NCRE) grillage tests previously cited provide data on two steel grillages whose ultimate failure was ascertained to have been caused primarily by longitudinal stiffener tripping. The pertinent scantlings (mean values) of the two grillages, identified as grillages 1a and 1b, were as follows:

Grillage	1a	1b
a =	48 in.	48 in.
b =	24 in.	24 in.
t =	0.315 in.	0.310 in.
d =	6.05 in.	6.0 in.*
t_w =	0.284 in.	0.28 in.*
f_w =	3.11 in.	3.0 in.*
t_f =	0.56 in.*	0.56 in.*

*Nominal values

Both grillages were nominally identical, the only difference being the presence of a 15 psi lateral loading on grillage 1b.

GRILLAGE 1a

Employing a modulus $E = 30 \times 10^6$ psi and a Poisson's ratio $\nu = 0.3$ the elastic tripping stress for grillage 1a according to Equation (70) with $C = 0$ and $m = 1$ is

$$(\sigma_e)_{cre} = 104.7 \text{ ksi} \qquad (C.1)$$

Substituting this value into Equation (100) with $\sigma_Y = 37$ ksi and $p_r \approx 0.5$ leads to an inelastic axial tripping stress

$$(\sigma_e)_{cr} = 33.7 \text{ ksi} \qquad (C.2)$$

PRECEDING PAGE BLANK

Since the classical elastic plate buckling stress, σ_{pbe}, given by Equation (94) is about 18.7 ksi, the assumption of the value $C = 0$ is thus seen to be correct and no iteration with regard to this parameter is necessary. Therefore, one may proceed directly to the calculation of the mean tripping stress $(\sigma_m)_{cr}$.

The calculation of the mean tripping stress requires the knowledge of the plating effective width b_e. Since the grillage at tripping has been loaded above the level of plate buckling, it is clear that the plating should be expected to be somewhat less than fully effective. Assuming[3] the following expression

$$\frac{b_e}{b} = \frac{2}{\beta} - \frac{1}{\beta^2} \tag{C.3}$$

where, in this case, β is a plate slenderness ratio

$$\beta = \frac{b}{t}\sqrt{\frac{\sigma_Y}{E}} \tag{C.4}$$

leads to a value of effective width

$$b_e \approx 0.607b = 14.6 \text{ in.} \tag{C.5}$$

Inserting this value into Equation (27) (with $(\sigma_e)_{cre}$ replaced by $(\sigma_e)_{cr}$) in turn provides the desired mean inelastic tripping stress,

$$(\sigma_m)_{cr} = 24.5 \text{ ksi} \tag{C.6}$$

This value compares quite favorably with the experimental value of 27.8 ksi measured at NCRE.

GRILLAGE 1b

Grillage 1b is nominally identical to 1a, differing only through the addition of a 15 psi lateral pressure. For this grillage, using Equation (70) with C = 0, m = 1, and the scantlings previously listed, the elastic axial tripping stress becomes

$$(\sigma_e)_{cre} = 99.4 \text{ ksi} \tag{C.7}$$

(Note that this value does not yet include the effects of lateral pressure and differs slightly from that of grillage 1a because of slight differences in the tabulated mean values of the various scantlings.) To include the effects of the lateral loading, the tripping load due to lateral loading alone is computed. Assuming an effective breadth of 50t for the combined plate-stiffener combination and then substituting the appropriate parameters and coefficients into Equation (46) results in a critical lateral loading for clamped ends, C = 0, and m = 1,

$$q_{cre} = +\ 17{,}100 \text{ lb/in.} \tag{C.8}$$

The applied lateral loading of 15 psi represents an effective line loading of 360 lb/in. for 24 in. frame spacing. Using the linear interaction Equation (84) the elastic axial tripping stress in the presence of lateral loading can now be computed,

$$\begin{aligned}(\sigma_e)_{cre,q} &= (\sigma_e)_{cre}\left(1 - \frac{q}{q_{cre}}\right)\\ &= 99.4\left(1 - \frac{360}{17{,}100}\right) \qquad \text{(C.9)}\\ &= 97.3 \text{ ksi}\end{aligned}$$

Since it is easily demonstrated that at failure the axial load is predominant, the inelastic tripping stress can now be calculated in the same manner as for grillage 1a, using Equation (100). This gives

$$(\sigma_e)_{cr,q} = 33.5 \text{ ksi} \tag{C.10}$$

Assuming the same expression for b_e/b as for grillage 1a, leads to a value of effective width

$$b_e \approx 0.600b = 14.4 \text{ in.} \tag{C.11}$$

and finally to the mean inelastic axial tripping stress

$$(\sigma_m)_{cr,q} = 24.1 \text{ ksi} \tag{C.12}$$

The corresponding experimental value from the NCRE tests is 27.1 ksi. Again agreement appears quite reasonable.

Although the agreement between analytical and experimental results appear quite encouraging, it is only fair to point out that several parameters whose values are difficult to define precisely can influence the predicted analytical values to varying degrees. The most significant, perhaps, is the choice of plating effective width which is necessary to determine "mean" from "peak" stresses. It can be demonstrated that, depending on the degree of plating effectiveness assumed, a rather wide range of mean tripping stress values can result. For example, in the case of grillage 1a, the inelastic axial tripping stress $(\sigma_e)_{cr}$ = 33.7 ksi, which is a peak stress, can produce mean tripping stress values $(\sigma_m)_{cr}$ as high as 33.7 ksi for fully effective plating to as low as 10.2 ksi for completely ineffective plating. The most appropriate value lies somewhere in between these extremes. Indicating that such wide ranges of predicted values can exist should not be interpreted as completely negating the value of the excellent agreement described here, rather it serves to point out that caution must be exercised in attempts at experimental correlation when limited amounts of data are available.

REFERENCES

1. Smith, C.S., "Compressive Strength of Welded Steel Ship Grillages," Journal of the Royal Institute of Naval Architects, No. 4 (Oct 1975).

2. Windenburg, D.F., "The Elastic Stability of Tee Stiffeners," United States Experimental Model Basin Report 457 (Nov 1938).

3. Evans, J.H., editor, "Ship Structural Design Concepts," Final Report on Project SR-200, Structural Design Criteria, Ship Structures Committee (1974).

4. Smith, C.S., "Bending, Buckling and Vibration of Orthotropic Plate-Beam Structures," Journal of Ship Research, Vol. 12, No. 4 (Dec 1968).

5. Wittrick, W.H., "General Sinusoidal Stiffness Matrices for Buckling and Vibration Analyses of Thin Flat-Walled Structures," International Journal of Mechanical Science, Vol. 10 (1968).

6. Bleich, F., "Buckling Strength of Metal Structures," McGraw-Hill Book Co., Inc., New York (1952).

7. Kavlie, D. and R.W. Clough, "A Computer Program for Analyses of Stiffened Plates Under Combined Inplane and Lateral Loads," University of California Report UCSESM 71-4 (Mar 1971).

8. "Design Data Sheet DDS100-4, Strength of Structural Members," Department of the Navy, Naval Ship Engineering Center (Aug 1969).

INITIAL DISTRIBUTION

Copies	
1	DDR&E/Library
1	CNO/OP 098T
1	CNR/Code 474
2	CHNAVMAT 1 MAT 08T23 1 Lib
1	USNA
1	NAVPGSCOL
1	USNROTCU & NAVADMINU MIT
1	DNL
1	NRL Tech Lib
16	NAVSEA 1 SEA 03R 1 SEA 312 1 SEA 312 (Aronne) 1 SEA 32 1 SEA 32R (Pohler) 1 SEA 321 1 SEA 322 1 SEA 323 1 SEA 323 (O'Brien) 1 SEA 323 (Arntson) 1 SEA 323 (Dye) 1 SEA 323 (Gallagher) 1 SEA 323 (Swann) 1 SEA 05R 1 SEA 05R (Vanderveldt) 1 SEA 996 (Tech Lib)
1	NAVAIRSYSCOM Str Br (Code 5302)
1	NAVOCEANSYSCEN
1	NAVSHIPYD BREMERTON WA
1	NAVSHIPYD CHARLESTON SC
1	NAVSHIPYD LONG BEACH CA
1	NAVSHIPYD PEARL HARBOR HI
1	NAVSHIPYD PHILADELPHIA PA
1	NAVSHIPYD PORTSMOUTH NH
1	NAVSHIPYD PORTSMOUTH VA
1	NAVSHIPYD VALLEJO CA
12	DDC
1	Wright-Patterson AFB Structures Div.
3	U.S. COGARD 1 Naval Eng Div. 1 Merchant Marine Tech Div. 1 Ship Structures Comm
1	Lib of Congress
2	MARAD 1 Div. of Ship Design 1 Off of Res and Dev
1	NSF Engr Div Lib
1	Univ of California, Berkeley Dept of Naval Arch
1	Catholic Univ Dept Mech Engr
1	George Washington Univ School of Engr & Applied Sci
1	Lehigh Univ/Dept Civil Engr

Copies	
1	Mass Inst of Tech Dept Ocean Engr
1	Univ of Michigan Dept NAME
1	Southwest Res Inst
1	Stevens Inst Tech Davidson Lab
1	Virginia Poly Inst & State Univ/Dept Engr Mech
1	Webb Inst
2	National Academy of Sci 1 National Res Council 1 Ship Hull Res Comm
1	SNAME
1	American Bureau of Shipping

CENTER DISTRIBUTION

Copies	Code	Name
1	17	
1	1706 (m)	
1	1720	
1	1730	
1	1730.1	
1	1730.2	
1	1730.3	
1	1730.4	
25	1730.5	
1	1730.6	
1	1740	
1	1750	
1	1770	
1	1770.7 (m)	
1	185	
10	5211.1	Reports Distribution
1	522.1	Unclassified Lib (C)
1	522.2	Unclassified Lib (A)

DTNSRDC ISSUES THREE TYPES OF REPORTS

1. DTNSRDC REPORTS, A FORMAL SERIES, CONTAIN INFORMATION OF PERMANENT TECHNICAL VALUE. THEY CARRY A CONSECUTIVE NUMERICAL IDENTIFICATION REGARDLESS OF THEIR CLASSIFICATION OR THE ORIGINATING DEPARTMENT.

2. DEPARTMENTAL REPORTS, A SEMIFORMAL SERIES, CONTAIN INFORMATION OF A PRELIMINARY, TEMPORARY, OR PROPRIETARY NATURE OR OF LIMITED INTEREST OR SIGNIFICANCE. THEY CARRY A DEPARTMENTAL ALPHANUMERICAL IDENTIFICATION.

3. TECHNICAL MEMORANDA, AN INFORMAL SERIES, CONTAIN TECHNICAL DOCUMENTATION OF LIMITED USE AND INTEREST. THEY ARE PRIMARILY WORKING PAPERS INTENDED FOR INTERNAL USE. THEY CARRY AN IDENTIFYING NUMBER WHICH INDICATES THEIR TYPE AND THE NUMERICAL CODE OF THE ORIGINATING DEPARTMENT. ANY DISTRIBUTION OUTSIDE DTNSRDC MUST BE APPROVED BY THE HEAD OF THE ORIGINATING DEPARTMENT ON A CASE-BY-CASE BASIS.